

**KNOCK PHENOMENON ANALYSIS ON A DIESEL-CNG DUAL
FUEL ENGINE USING EXPERIMENTAL FUEL RATIO**

MUAMMAR MUKHSIN BIN ISMAIL



PTTA UTHM
PERPUSTAKAAN TUNKU TUN AMINAH

UNIVERSITI TUN HUSSEIN ONN MALAYSIA

UNIVERSITI TUN HUSSEIN ONN MALAYSIA

**STATUS CONFIRMATION FOR THESIS
DOCTOR OF PHILOSOPHY**

**KNOCK PHENOMENON ANALYSIS ON A DIESEL-CNG DUAL FUEL
ENGINE USING EXPERIMENTAL FUEL RATIO**

ACADEMIC SESSION: 2020/2021

I, **MUAMMAR MUKHSIN BIN ISMAIL**, agree to allow Thesis to be kept at the Library under the following terms:

1. This Thesis is the property of the Universiti Tun Hussein Onn Malaysia.
2. The library has the right to make copies for educational purposes only.
3. The library is allowed to make copies of this Thesis for educational exchange between higher educational institutions.
4. The library is allowed to make available full text access of the digital copy via the internet by Universiti Tun Hussein Onn Malaysia in downloadable format provided that the Thesis is not subject to an embargo. Should an embargo be in place, the digital copy will only be made available as set out above once the embargo has expired.
5. ** Please Mark (v)

CONFIDENTIAL (Contains information of high security or of great importance to Malaysia as STIPULATED under the OFFICIAL SECRET ACT 1972) *Title and Abstract only*

RESTRICTED (Contains restricted information as determined by the organization/institution where research was conducted)-
Title, Abstract and Introduction only

EMBARGO _____ until _____
(date) (date)

FREE ACCESS

Approved by,

MUAMMAR MUKHSIN BIN ISMAIL

ASSOC. PROF. DR. MAS FAWZI BIN MOHD ALI

Permanent Address:

TM11, KAMPUNG TALANG MASJID,
33000 KUALA KANGSAR,
PERAK

Date : 16/1/2021

Date: 16/1/2021

NOTE: ** If this Thesis is classified as CONFIDENTIAL or RESTRICTED, please attach the letter from the relevant authority/organization stating reasons and duration for such classification.

This thesis has been examined on date 25th December 2020
and is sufficient in fulfilling the scope and quality for the purpose of awarding the
Degree of Doctor of Philosophy

Chairperson:

ASSOC. PROF. IR. DR. SIA CHEE KIONG
Faculty of Mechanical and Manufacturing Engineering
Universiti Tun Hussein Onn Malaysia

Examiners:

PROF. DR. YOSHIYUKI KIDOGUCHI
Department of Mechanical Engineering
Tokushima University, Japan

ASSOC. PROF. DR. MOHAMMAD KAMIL BIN ABDULLAH
Faculty of Mechanical and Manufacturing Engineering
Universiti Tun Hussein Onn Malaysia



PTTA UTHM
PERPUSTAKAAN TUNKU TUN AMINAH

KNOCK PHENOMENON ANALYSIS ON A DIESEL-CNG DUAL FUEL
ENGINE USING EXPERIMENTAL FUEL RATIO

MUAMMAR MUKHSIN BIN ISMAIL

This thesis is submitted to fulfil part of the requirement for the award of the
Doctor of Philosophy of Mechanical Engineering



PTTA UTHM
PERPUSTAKAAN TUNKU TUN AMINAH

Faculty of Mechanical and Manufacturing Engineering
Universiti Tun Hussein Onn Malaysia

JANUARY 2021

I hereby declare this work in this thesis is my own except for quotation and summaries which have been duly acknowledge

Student : _____

MUAMMAR MUKHSIN BIN ISMAIL

Date : 16/1/2021

Supervisor : _____

ASSOC. PROF. DR. MAS FAWZI BIN MOHD ALI

Co Supervisor : _____

ASSOC. PROF. DR. SHAHRUL AZMIR BIN OSMAN

Co Supervisor : _____

ASST. PROF. DR. JUNTAKAN TAWEEKUN



PTTA UTHM
PERPUSTAKAAN TUNKU TUN AMINAH

DEDICATION

This thesis is dedicated to:

My beloved family and teacher who have raised me to be the person I am today.

Tomorrow researcher and scholar.

*So, verily, with every difficulty, there is a relief.
Verily, with every difficulty there is a relief.
(Quran Al-Kareem 54:5-6)*



PTTA UTHM
PERPUSTAKAAN TUNKU TUN AMINAH

ACKNOWLEDGEMENT

All praise and thanks belong to Allah for granting me the strength to complete this thesis.

I would like to express my sincere thanks and deep gratitude to my supervisor, Assoc. Prof. Dr. Mas Fawzi bin Mohd Ali, for his guidance along the six years since my bachelor's degree in 2015. His excellent advice and critics push my vision beyond the limit. Sincere thanks to my co-supervisors, Assoc. Prof. Dr. Shahrul Azmir bin Osman and Asst. Prof. Dr. Juntakan Taweekun for their advice, encouragement, and support.

I wish to express my appreciation to Tc. Mzahar Bin Abd Jalal and Mr. Aimizil Hamarul Farid bin Haji Mazlan for their invaluable assistance and advice to accomplish this project. An appreciation also to my fellow research group members Mr. Mustaqim bin Tukiman, Mr. Khairul Ilman bin Sarwani, Mr. Putera Mohamad Adam bin Amat Azman, Ts. Dr. Norrizal bin Mustaffa, Ts. Dr. Abd. Fathul Hakim bin Zulkifli, Dr. Rais Hanizam bin Madon, Mr. Anwar Syahmi bin Adlin Zafrulan, and Mdm. Siti Natasha binti Malik Fesal for their direct contribution along this journey.

Last but not least, my deepest gratitude to my parents and family for their unconditional support and understanding.



PTT AUTHM
PERPUSTAKAAN TUNJUNG AMINAH

ABSTRACT

Knock avoidance is crucial to establish a proper Diesel-CNG Dual Fuel (DDF) engine. The causes of this phenomenon are still vague due to the lack of knock detection and characterization methods available. This study presents a knock characterization technique using a statistical analysis based on engine block vibration signal. Several experiments were conducted on a 2.5-litre converted DDF engine running at a constant engine speed between 1400 rpm and 3000 rpm with several diesel to CNG fuel ratio. This study found that when the diesel to CNG fuel ratio reached 70:30 at 1800 rpm to 3000 rpm, and 60:40 at 1400 rpm and 1600 rpm, engine knock was detected. A knock index was calculated from the vibration signal using Band-pass, Rectify, Integrate, and Compare (BRIC) method to determine knock intensity for each engine cycle. A three-sigma rule was applied to determine the threshold level of knock occurrence at the tested engine speeds. The knock thresholds at 1400 rpm, 1600 rpm, 1800 rpm, 2000 rpm, 2200 rpm, 2400 rpm, 2600 rpm, 2800 rpm, and 3000 rpm were found to have a knock index of 3.72, 3.49, 3.21, 2.71, 2.27, 1.80, 2.02, 1.80, and 1.73 respectively. Using a 5% knock cycle occurrence within the third and sixth standard deviation as a deciding criteria, a knock quality level was categorised as a vague, light, medium, and heavy knock. The analysed result shows that a severe knock occurred due to a sudden transition between a low and high knock intensity in a consecutive engine cycle, which yields a non-periodic mechanical shock. The calculated coefficient of variation of the knock index (COV_{KI}) shows that the severe knock occurred when the COV_{KI} is 0.30 and above. It suggests that the knock phenomenon on a DDF engine occurs due to an abrupt heat release rate during the mixing-controlled combustion phase and micro-explosion during the late combustion phase.

ABSTRAK

Fenomena ketukan perlu dicegah untuk menghasilkan enjin dwi bahan api diesel-CNG (DDF) yang sempurna. Punca berlakunya fenomena ini masih lagi samar disebabkan kurangnya kaedah pengesanan dan penciriannya. Kajian ini menghuraikan teknik pencirian fenomena ketukan menggunakan analisa statistik berdasarkan isyarat dari getaran bongkah enjin. Beberapa ujikaji telah dijalankan keatas enjin DDF berkapasiti 2.5-liter pada kelajuan malar diantara 1400 rpm dan 3000 rpm dengan beberapa nisbah bahan api diesel kepada CNG. Kajian ini telah menemui bahawa fenomena ketukan berlaku apabila nisbah bahan api diesel kepada CNG mencapai 70:30 pada 1800 rpm ke 3000 rpm, dan 60:40 pada 1400 rpm dan 1600 rpm. Indeks ketukan telah dikira menggunakan kaedah *Band-pass, Rectify, Integrate, dan Compare* (BRIC) daripada isyarat getaran bongkah enjin untuk menentukan kekuatan ketukan untuk setiap kitaran enjin. Peraturan tiga-sigma telah diguna pakai untuk menentukan nilai ambang fenomena ketukan yang berlaku pada setiap kelajuan putaran enjin. Nilai ambang yang ditemui pada 1400 rpm, 1600 rpm, 1800 rpm, 2000 rpm, 2200 rpm, 2400 rpm, 2600 rpm, 2800 rpm, dan 3000 rpm masing-masing berada pada indeks ketukan 3.72, 3.49, 3.21, 2.71, 2.27, 1.80, 2.02, 1.80, dan 1.73. Tahap kekuatan ketukan telah dikelaskan kepada samar, perlahan, sederhana, dan kuat menggunakan kriteria 5% kitar ketukan yang berlaku di dalam setiap sisihan piawai ketiga hingga keenam. Hasil analisa menunjukkan bahawa ketukan yang teruk berlaku disebabkan oleh perubahan mengejut antara ketukan berkekuatan perlahan dan kuat di dalam suatu kitar enjin yang berterusan, yang mana ianya membentuk suatu kejutan mekanikal yang tidak menentu. Pekali variasi indeks ketukan (COV_{KI}) menunjukkan bahawa ketukan yang teruk berlaku apabila nilai COV_{KI} pada 0.30 dan keatas. Hasil penelitian juga mencadangkan bahawa fenomena ketukan yang berlaku pada enjin DDF adalah disebabkan oleh peningkatan kadar pelepasan haba yang mendadak ketika fasa pembakaran pencampuran-terkawal dan letupan mikro ketika fasa hujung pembakaran.

CONTENTS

	DECLARATION	ii
	ACKNOWLEDGEMENT	vii
	ABSTRACT	viii
	ABSTRAK	ix
	CONTENTS	x
	LIST OF TABLES	xii
	LIST OF FIGURES	xiv
	ABBREVIATIONS AND NOMENCLATURES	xix
	LIST OF APPENDICES	xxii
CHAPTER 1	INTRODUCTION	1
	1.1 Background of Study	1
	1.2 Problem Statement	3
	1.3 Objectives	3
	1.4 Scopes of Study	4
	1.5 Significance of the Study	4
CHAPTER 2	LITERATURE REVIEW	5
	2.1 Diesel Engine	5
	2.2 Diesel Fuel	8
	2.3 CNG as Alternative Fuel	10
	2.4 DDF Engine	13
	2.4.1 DDF Engine Performance	14
	2.4.2 DDF Engine Combustion	18
	2.5 Knock Phenomenon	26
	2.5.1 Knock Detection Method	32
	2.5.2 Knock Phenomenon on DDF Engine	38
	2.6 Summary of Literature Review	42



CHAPTER 3	METHODOLOGY	44
3.1	Study Flow Diagram	44
3.2	Experiment Setup	46
3.2.1	Test Subject	47
3.2.2	Test Fuel Specimen	49
3.2.3	Dynamometer	51
3.2.4	Engine System Monitoring	52
3.2.5	Combustion Analyser	54
3.2.6	Diesel Fuel Mass Flow Rate	59
3.2.7	CNG Fuel Mass Flow Rate	61
3.2.8	Intake and Exhaust Temperature	63
3.2.9	Engine Knock Signal	65
3.3	Knock Phenomenon Determination	66
3.4	Knock Cycle Determination	69
3.5	Experiment Matrix	75
3.6	Experiment Standard Operation Procedure	77
CHAPTER 4	RESULT AND DISCUSSION	81
4.1	Diesel to CNG Fuel Ratio Limit on a DDF Engine	81
4.2	Knock Phenomenon Classification on a DDF Engine	83
4.3	Effect of Fuel Ratio to the Knock Phenomenon	106
4.4	Effect of Engine Speed to the Knock Phenomenon	111
4.5	Effect of Intake Temperature to the Knock Phenomenon	113
4.6	Summary of the Knock Phenomenon	115
CHAPTER 5	CONCLUSION AND RECOMMENDATION	118
5.1	Conclusion	118
5.2	Contribution of the Study	119
5.3	Recommendation	120
	REFERENCES	121
	APPENDIX	136



LIST OF TABLES

2.1	Diesel fuel properties by various blends in Malaysia (Malaysian Standard, 2014; Petron Malaysia, 2014; Petronas Dagangan Berhad, 2005)	10
2.2	In-cylinder pressure and heat release rate comparison of a DDF engine to diesel engine (Lounici et al., 2014; Selim, 2001)	19
3.1	Specification of Toyota Hilux 2.5 Direct Injection Diesel equipped with DDF system (Ismail et al., 2016; Toyota Motor Corporation, 2007)	48
3.2	Diesel fuel properties as manufactured by Petron Malaysia (Petron Malaysia, 2014)	50
3.3	Natural gas properties as manufactured by Gas Malaysia (Gas Malaysia, 2015)	50
3.4	Kistler M5 PiezoStar® Cylinder Pressure Sensor 6056A	54
3.5	Kistler 1 Channel Charge Amplifier 5018A specification	56
3.6	Dewetron Dewe-Crank Angle CPU specification	57
3.7	National Instruments data acquisition specification	58
3.8	Specification of Ono Sokki FZ-2100 Massflow Meter (Ono Sokki, 2010)	60
3.9	Specification of Gas Flow Meter (Alicat Scientific, 2016)	62
3.10	Pico Technology 8-Channel Thermocouple Data Logger TC-08 specification	64
3.11	Experiment matrix	76
3.12	Fuel mass flow rate ratio across 1400 rpm to 3000 rpm	77



3.13	Equipment parameter setup	78
4.1	Knock phenomenon observation during the experiment	82
4.2	Knock occurrence percentages over 500 engine cycles	85
4.3	Diesel injection timing against fuel ratio and engine speed	97
4.4	Knock category and its expression for vague, light, medium, and heavy knock	100
4.5	$\%N_x$ above the third standard deviation from the mean	101
4.6	$\%N_x$ above the fourth standard deviation from the mean	101
4.7	$\%N_x$ above the fifth standard deviation from the mean	102
4.8	$\%N_x$ above the sixth standard deviation from the mean	102
4.9	Knock classification for various fuel ratios across the engine speed	103
4.10	COV_{KI} for various fuel ratios across engine speed	104



LIST OF FIGURES

2.1	Diesel common-rail direct injection system diagram	6
2.2	Evolution of diesel common-rail technologies and European Emission Standard Compliance	7
2.3	Diesel sulphur content according to the European Emission Standard	9
2.4	Natural gas layer in petroleum well	11
2.5	World proven natural gas reserves and demand (IEA, 2018; OPEC, 2018)	12
2.6	Total BSFC against engine load at various engine speeds (Lounici et al., 2014)	15
2.7	BSEC between the DDF engine and diesel engine (Ismail et al., 2018)	16
2.8	BTE at various CNG fuel fractions (Karagöz et al., 2016)	17
2.9	DDF engine efficiency and smoke emission across IMEP and fuel ratio (Vávra et al., 2017)	18
2.10	In-cylinder pressure and heat release rate for diesel engine and DDF engine (Lounici et al., 2014)	19
2.11	Pressure rise rate against pilot injection timing for diesel and DDF engine (Selim, 2001)	20
2.12	DDF combustion against CNG fuel fraction (Wannatong et al., 2007)	22
2.13	In-cylinder pressure at various fuel ratios in a constant volume chamber (Firmansyah et al., 2017)	22
2.14	Photography image of the DDF and diesel fuel combustion (Firmansyah et al., 2015, 2017)	23

2.15	DDF engine combustion at various equivalence ratios (Shioji et al., 2001)	24
2.16	Diesel injector tip temperature against CNG fuel fraction at stoichiometric condition (Vávra et al., 2017)	25
2.17	New diesel injector and fouled injector comparison due to stoichiometric combustion with high CNG fuel fraction (Vávra et al., 2017)	25
2.18	Knock phenomenon effect on engine damage (Wang, Liu, et al., 2015)	27
2.19	Number of work published on the SAE International relate to the knock phenomenon	28
2.20	Comparison between normal combustion, conventional knock and super-knock (Wang et al., 2014; Wang, Liu, et al., 2015)	29
2.21	Pre-ignition to super-knock process (Wang et al., 2017; Wang, Qi, et al., 2015)	30
2.22	Combustion characteristics of gasoline and diesel engine (Priede, 1980)	31
2.23	In-cylinder pressure with a normal, slight knock and intense knock combustion (Douaud & Eyzat, 1977)	33
2.24	In-cylinder pressure and knock intensity (Chun & Heywood, 1989)	34
2.25	Process flow for knock detection using MAPO and PTP (M.S. Lounici et al., 2017)	35
2.26	Process flow for knock detection using ND method	35
2.27	Comparison of knock detection between MAPO and ND methods (Bares et al., 2018)	36
2.28	In-cylinder pressure, knock sensor and ion sensor trace for knock detection (Ängeby et al., 2018)	37
2.29	Heat release rate and combustion duration by various CNG substitution (Firmansyah et al., 2015)	39
2.30	Knock intensity by the various start of combustion and combustion duration (Sremec et al., 2017)	40



PTT AUTHM
PERPUSTAKAAN TUN AMINAH

2.31	CNG auto-ignition region by various equivalence ratios against intake temperature and pressure (Jun et al., 2003)	41
2.32	Effect of the knock phenomenon on piston and engine liner (Wannatong et al., 2007)	42
3.1	Study Flow Diagram	45
3.2	Experiment testbed setup	46
3.3	Toyota Hilux 2.5 direct injection diesel with common-rail	47
3.4	DDF system installation diagram (Ismail et al., 2016)	49
3.5	Dynapack 4WD Chassis Dynamometer which was used for the experimental works	51
3.6	Bosch KTS 570 diagnostic tool	52
3.7	Bosch KTS 570 diagnostic tool assembly diagram	53
3.8	ESI[tronic] 2.0 software interface	53
3.9	Combustion analyser assembly	54
3.10	Kistler M5 PiezoStar® Cylinder Pressure Sensor 6056A and its installation	55
3.11	Kistler 1 Channel Charge Amplifier 5018A and its display	56
3.12	Dewe-Crank Angle CPU and installation location of Dewe-RIE encoder	57
3.13	National Instruments data acquisition	58
3.14	Ono Sokki FZ-2100 and FM-2500 for measuring diesel mass flow rate	89
3.15	Schematic diagram for assembling Ono Sokki Massflow Meter on the diesel fuel line	60
3.16	Alicat Scientific M-250SLPM Mass Gas Flow Meter and its display	61
3.17	Alicat Scientific M-250SLPM Mass Gas Flow Meter assembly diagram	62
3.18	Pico Technology 8-Channel Thermocouple Data Logger TC-08 and unsheathed K-Type thermocouple probe	63



3.19	Thermocouple installation location	64
3.20	Engine knock recorder system assembly diagram	65
3.21	Audio recording system assembly diagram	66
3.22	Interface of REAPER Digital Audio Workstation software	67
3.23	Waveform between normal and knock operation at 1400 rpm engine speed	68
3.24	Knock index calculation process	69
3.25	Raw knock signal with its spectrum	70
3.26	Filtered knock signal within 0.125 Hz to 0.375 Hz bandwidth	71
3.27	Selected location of combustion and non-combustion segment	72
3.28	Approximated population percentage in a normal distribution histogram	74
3.29	Example of the knock cycle determination	75
4.1	Knock index histogram for the 100D fuel ratio with various engine speeds	84
4.2	Knock index distribution at 1400 rpm engine speed	86
4.3	Knock index distribution at 1600 rpm engine speed	87
4.4	Knock index distribution at 1800 rpm engine speed	88
4.5	Knock index distribution at 2000 rpm engine speed	89
4.6	Knock index distribution at 2200 rpm engine speed	90
4.7	Knock index distribution at 2400 rpm engine speed	91
4.8	Knock index distribution at 2600 rpm engine speed	92
4.9	Knock index distribution at 2800 rpm engine speed	93
4.10	Knock index distribution at 3000 rpm engine speed	94
4.11	Knock index boxplot for various fuel ratios and engine speeds	95
4.12	Heat release rate average for 100D fuel ratio against engine speed	95
4.13	HC and CO emission for various fuel ratios against engine speed	96



4.14	Pre-combustion occurrence for the 60D40G fuel ratio at 1400 rpm engine speed	98
4.15	Knock index distribution for 60D40G fuel ratio at 1400 rpm and 70D30G fuel ratio at 1800 rpm engine speed	105
4.16	Knock signal and combustion at 1600 rpm engine speed	107
4.17	Knock signal and combustion at 2800 rpm engine speed	109
4.18	Heat release rate at a low-speed and high-speed engine operation with the 100D and 70D30G fuel ratios	112
4.19	Knock index distribution during the knock phenomenon occurrence	113
4.20	Intake temperature at the 70D30G fuel ratio at 2800 rpm engine speed	114



ABBREVIATIONS AND NOMENCLATURES

AFR	-	Air-Fuel Ratio
AKI	-	Anti-knock Index
B2	-	Diesel blended with 2% Fatty Acid Methyl Ester
B5	-	Diesel blended with 5% Fatty Acid Methyl Ester
B7	-	Diesel blended with 7% Fatty Acid Methyl Ester
B10	-	Diesel blended with 10% Fatty Acid Methyl Ester
BMEP	-	Brake Mean Effective Pressure
BRIC	-	Band-pass, Rectify, Integrate and Compare
BSEC	-	Brake Specific Energy Consumption
BSFC	-	Brake Specific Fuel Consumption
BTE	-	Brake Thermal Efficiency
C_2H_6	-	Ethane
C_3H_8	-	Propane
C_4H_{10}	-	Butane
C_5H_{12}	-	Pentane
$C_6+(C_6H_{14})$	-	Hexane
CA	-	Crank Angle
CEEMD	-	Complimentary Ensemble Empirical Mode Decomposition
CH_4	-	Methane
CI	-	Compression-Ignition
CNG	-	Compressed Natural Gas
CO	-	Carbon Monoxide
CO_2	-	Carbon Dioxide
COV	-	Coefficient of Variation
COV_{KI}	-	Coefficient of Variation of Knock Index
CV	-	Calorific Value

DDF	-	Diesel-CNG Dual Fuel
DIN	-	Deutsche Industrie Norm
ECU	-	Engine Control Unit
EFI	-	Electronic Fuel Injection
EGR	-	Exhaust Gas Recirculation
EPA	-	Environmental Protection Agency
FFT	-	Fast Fourier Transform
HC	-	Hydrocarbon
HCCI	-	Homogeneous Charge Compression Ignition
HRR	-	Heat Release Rate
H ₂ O	-	Dihydrogen Monoxide
Hz	-	Hertz
IEA	-	International Energy Agency
IMEP	-	Indicated Mean Effective Pressure
KI	-	Knock Index
KOH	-	Potassium Hydroxide
LFE	-	Laminar Flow Element
LFL	-	Lower Flammable Limit
LHV	-	Lower Heating Value
MAPO	-	Maximum Amplitude Pressure Oscillation
MPa	-	Mega Pascal
ND	-	New Definition
NI-CAS	-	National Instruments Combustion Analysis System
NO _x	-	Nitrogen Oxide
O ₂	-	Oxygen
OBD	-	On-Board Diagnostic
OPEC	-	Organization of the Petroleum Exporting Country
PME	-	Palm Methyl Ester
ppm	-	Parts Per Million
pS/m	-	Pico Siemens per meter (Conductivity)
PTP	-	Peak-to-Peak
rpm	-	Revolution Per Minute
SAE	-	Society of Automotive Engineers



SI	-	Spark Ignition
SLPC	-	Short-Lived Climate Pollutants
SLPM	-	Standard Litre per Minute
TDC	-	Top Dead Centre
UFL	-	Upper Flammable Limit
ULSD	-	Ultra-Low Sulphur Diesel
WHO	-	World Health Organization
\dot{m}	-	Mass Flow Rate
$^{\circ}\text{C}$	-	Degree Celsius
$^{\circ}\text{CA}$	-	Degree Crank Angle
$\%_{knock}$	-	Percentages of Knock Cycle Occurrence
$\%N_x$	-	Knock Index Population
μ	-	Mean
σ	-	Standard Deviation
ϕ	-	Equivalence Ratio



PTTA UTHM
PERPUSTAKAAN TUNKU TUN AMINAH

LIST OF APPENDICES

A	List of Publications	136
B1	Test bed setup in a dynamometer room	138
B2	Test bed setup diagram	139
B3	Thermocouple probe installation location	140
B4	Crank angle encoder assemblies	140
B5	Custom made disc encoder with 360 slits drawing	141
C1	Diesel fuel product data sheet	143
C2	CNG fuel safety data sheet page 1	144
C3	CNG fuel safety data sheet page 2	145
C4	CNG fuel safety data sheet page 3	146
C5	CNG fuel safety data sheet page 4	147
C6	CNG fuel safety data sheet page 5	148
C7	CNG fuel safety data sheet page 6	149
C8	CNG fuel safety data sheet page 7	150



PTFAUTHM
PERPUSTAKAAN TUN AMINAH

CHAPTER 1

INTRODUCTION

1.1 Background of Study

Organization of the Petroleum Exporting Country (OPEC) has reported that the proven crude oil reserve had increased in 2017 (OPEC, 2018). Along with that, the International Energy Agency (IEA) has reported the fuel consumption in the transportation sector has been drastically growing for a few decades from 1980 to 2015. In accordance with the projection, the growth will continuously increase by 1.2 % annually until 2022 (IEA, 2017).

Fossil fuel combustion emits harmful pollution. Some of the emissions are poisonous and causing serious health problems through direct exposure. The rest of the non-poisonous emissions affect health indirectly through climate change. As reported in 2017, about tens of thousands of death are estimated every year caused by climate change (WHO, 2017).

Air pollution from the transportation sector has been listed as Short-Lived Climate Pollutants (SLPC), which contributes to global warming and climate change (WHO, 2015). Based on these issues, most of the developed countries, especially the United Kingdom and the United States have ruled some policies to mitigate this matter. In the United Kingdom, renewable energy regulation was proposed in 2001 and focused on electricity generation. The regulation was amended in 2009 by including the biofuel consumption for a vehicle (European Union, 2001, 2009a). Energy Policy Act of 2005 was introduced in the United States to enhance the utilization of efficient and renewable energy (42 USC 15801, 2005). This policy provides an incentive to the



program regarding renewable and efficient energy. Continuing from this policy, Environmental Protection Agency (EPA) launched the Renewable Fuel Standard Program in 2010 to replace the existing fuel programs. This program highlights the standard of biofuel used and has been amended to enhance sustainable energy utilization (40 CFR Part 80, 2010, 2012a, 2012b, 2013, 2016, 2017).

Global implementation of the sustainable energy policy will reduce fossil fuel demand. However, an encouraging increment of the world's proven natural gas resources may lead to over-abundance. A study done by IEA in 2017 was showed that the natural gas supply and demand could be rebalanced by making a new policy to enhance the natural gas demand by switching coal and oil utilization to natural gas in the power, industrial, and transportation sectors (IEA, 2018).

Compressed Natural Gas (CNG) is a flexible fuel and suitable for various types of energy generators and has been used as the alternative for an internal combustion engine. Its application on a Spark Ignition (SI) engine is straight forward by installing an additional gas fuel system and promotes lower carbon emission than the gasoline fuel. However, its application on a diesel engine is not straight forward. A high octane rating of the CNG fuel needs a source of ignition for combustion. The dedicated Compression Ignition (CI) engine is converted to the SI engine by a major modification, but it demands a high initial cost and effort. Thus, a Diesel-CNG Dual Fuel (DDF) system is preferred to be applied by installing an additional gas fuel system on the diesel engine. This system operates by injecting the CNG fuel inside the cylinder and ignited by a small portion of the diesel fuel.

According to the author's previous study, the DDF engine promotes lower Carbon Dioxide (CO₂) and Nitrogen Oxide (NO_x) emission with comparable performance than the diesel engine. However, its Hydrocarbon (HC) emission was typically higher than the diesel engine and increased against the CNG fuel quantity increment (Ismail et al., 2018). Yet, several studies found that the over-increment of the CNG fuel quantity led to the knock phenomenon occurred and resulting in the engine damage (Wannatong et al., 2007).



1.2 Problem Statement

The knock phenomenon is a part of the obstacle to establishing a DDF engine. It occurs when the CNG fuel quantity exceeds a certain limit in the diesel to CNG fuel ratio. Although this phenomenon is audible, its occurrence is difficult to be seen via combustion analysis from the in-cylinder pressure signal because it occurs at high speed and a certain bandwidth. Thus, the root cause of its occurrence when the CNG fuel exceeds the limit is still vague and uncharacterised due to the limitation of available technology. Various knock detection methods were proposed by post-processing in-cylinder pressure trace, engine vibration signal, and ion signal even with mathematical analysis. However, those methods were complex, needs high-resolution equipment, and prone to false detection especially if it occurs at a low-intensity. Up to now, the best knock detection method is still unclear (Gómez Montoya et al., 2018). Therefore, in this work, an alternative knock detection method using an engine vibration signal with a statistical approach was evaluated, and the causes of the knock phenomenon on the DDF engine can be investigated to find opportunities for further improvement.

1.3 Objectives

The objectives of this study are:

- i. To determine diesel to CNG fuel ratio limits on a DDF engine before the knock occurrence.
- ii. To evaluate the use of the statistical method to index the knock phenomenon.
- iii. To classify the knock phenomenon of a DDF engine combustion using standard deviation.
- iv. To propose the probable causes of the knock phenomenon occurrence on a DDF engine.

1.4 Scopes of Study

The scopes of this study are as below:

- i. The engine studied is a 4-cylinder 2.5-litre diesel engine with common-rail direct injection (2KD-FTV). Two gas injectors are installed on the intake manifold.
- ii. The diesel to CNG fuel mass ratio tested are 90:10, 80:20, 70:30, and 60:40, or until the knock phenomenon onset within the operating range from 1400 rpm to 3000 rpm engine speed on a chassis dynamometer.
- iii. The total fuel mass flow rate is set according to the 0.7 equivalence ratio.

1.5 Significance of the Study

This study evaluates an alternative knock detection method using statistics and analyses probable causes of the knock phenomenon occurrence on a DDF engine. The findings of this study can be applied to detect, predict, and prevent knock phenomenon occurrence on any fuel converted engine; and also to improve the DDF engine combustion. This study may also be a jumping-off point towards mitigating climate change through a low carbon emission by the DDF engine.



CHAPTER 2

LITERATURE REVIEW

2.1 Diesel Engine

A diesel engine was invented by Rudolf Diesel in 1897, which was the golden era of the coal steam engine. It was designed to provide a higher brake power with greater efficiency than the steam engine. An early diesel engine uses a governor to regulate the desired fuel quantity. The fuel is premixed with air in the intake manifold before entering the cylinder. The air-fuel mixture is compressed to generate heat inside the cylinder. When it reaches its certain limit temperature, the fuel is auto-ignited and spontaneously combusted.

Ideal combustion of the diesel engine should produce only CO₂ and Dihydrogen Monoxide (H₂O) emissions; however, it is hard to be achieved in actual combustion due to it being affected by several conditions. The diesel fuel presence is in a liquid form and not homogeneously mixed with air. It yields a non-uniform local air-fuel ratio region in the cylinder. When the combustion occurs, the flame propagates to the combustible air-fuel ratio zone either in a lean, stoichiometric, or rich zone. The local rich air-fuel ratio zone has a lack of oxygen content, forms soot and Carbon Monoxide (CO) emission due to poor oxidization of air-fuel mixture. Therefore, the diesel engine is operated in a lean air-fuel ratio below equivalence ratio 0.8 to keep soot formation below a tolerable limit.

Diesel engine technology has been continuously improved to reduce hazardous emissions. Emission standard regulation has also been implemented to protect the environment and health from the internal combustion engine emissions. A well-known



emission standard is the European Emission Standard which has been implemented since 1970. In 1992, the regulation was amended and known as EURO 1, which controls the limit of CO, NO_x and soot emissions from the vehicle. The regulation has been continuously amended following the needs, the capability of current vehicle technology and the capability of fuel. After several amendments, the current emission regulation is EURO 6 and has been implemented since 2014.

Today, diesel engine technology has gone further by lowering its emissions and improving its efficiency. The diesel common-rail direct injection system was introduced in 1995 and pioneered by Denso Corporation. The system was electronically controlled and adapted from the gasoline Electronic Fuel Injection (EFI) system, as shown in Figure 2.1. A high-pressure diesel fuel is supplied by a high-pressure pump into the fuel rail. The fuel pressure is regulated by a pressure limiter and a suction control valve to ensure consistency of fuel pressure supplied. The fuel injector is controlled by an Engine Control Unit (ECU), and the fuel is directly injected into the cylinder. This system is able to supply a highly-pressurized fuel consistently at entire engine speed so that a proper combustion can occur since the cold start.

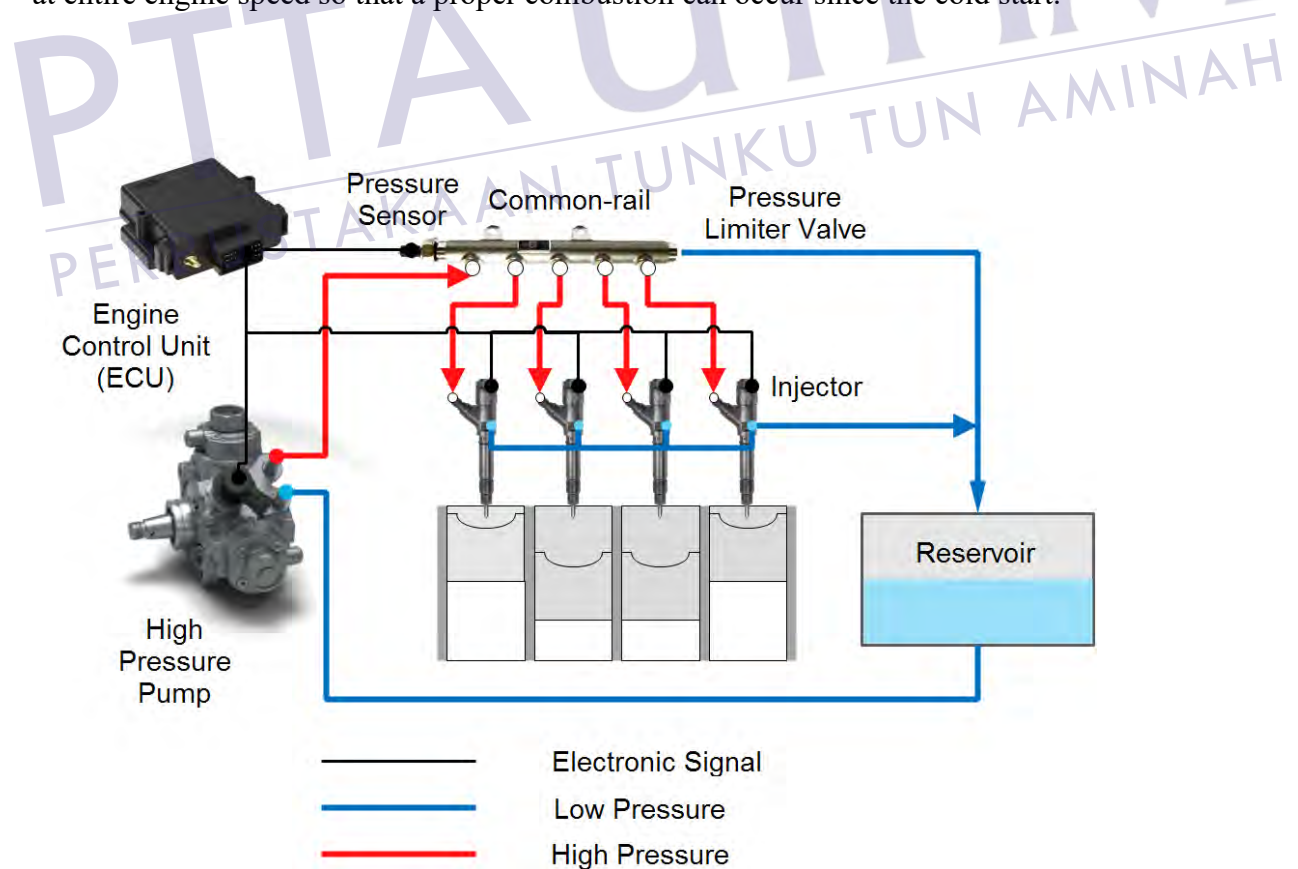


Figure 2.1: Diesel common-rail direct injection system diagram

Since it was introduced in 1995, the diesel common-rail technology was expanded and followed by Bosch and Delphi, which were the well-known company in the automotive industry. The evolution of diesel common-rail technology is still ongoing and focusing on lower fuel consumption and CO₂ emission to comply with the current emission regulation. The improvement has been made by increasing its operating pressure and fuel injection strategy so that it increases its efficiency. Today, the current diesel common-rail system is capable to operate up to 300 MPa, as shown in Figure 2.2. Several data in Figure 2.2 were collected from Flaig et al. (1999), Dohle et al. (2004), Koji Nagata (2004), Nagata et al. (2004), Kumano et al. (2006) and Matsumoto et al. (2013).

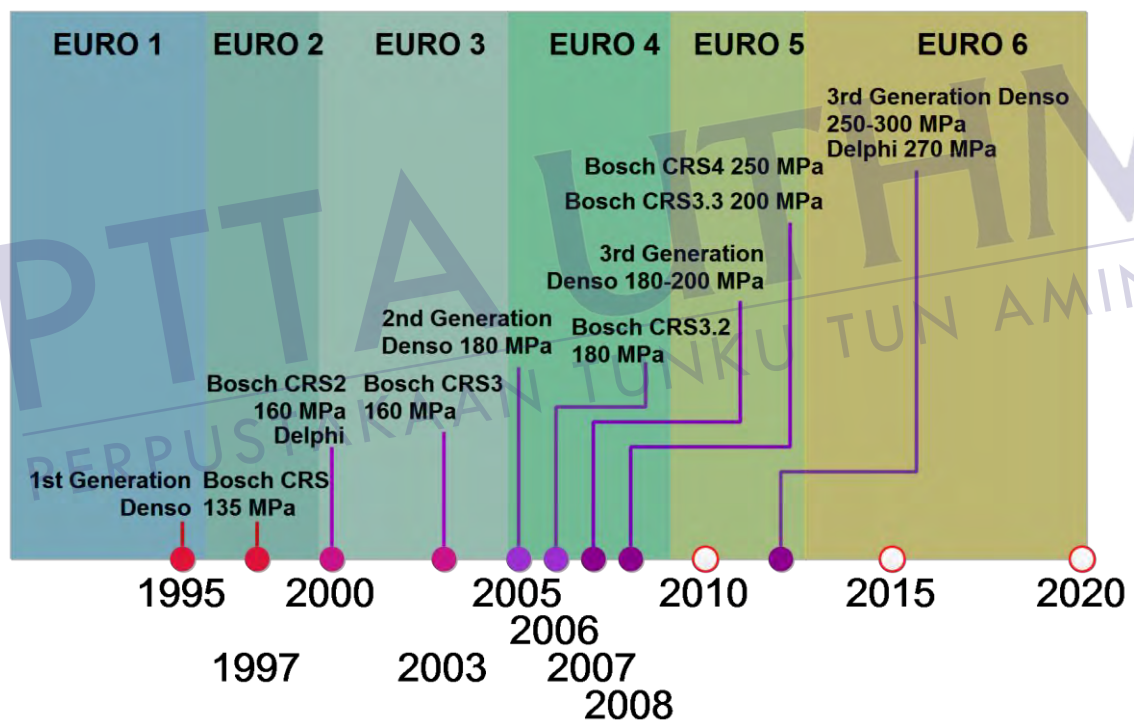


Figure 2.2: Evolution of diesel common-rail technologies and European Emission Standard Compliance

2.2 Diesel Fuel

Diesel fuel is distilled from the crude petroleum oil. It is less volatile and has higher energy density compared to petrol fuel. Thus, it releases more energy per volume and provides better fuel economy than petrol. Diesel fuel is commonly used in a compression ignition engine and characterized by its Cetane number. It is corresponding to the period of fuel to self-ignite and indexed on a special compression ignition engine. The higher Cetane number represents the shorter period of ignition delay.

Diesel fuel has high sulphur content and pollutes the environment. The oxidization of sulphur during the combustion potentially produces sulphuric acid when it combines with water vapour (from the combustion or atmospheric) and contributes to the acid rain. The amount of sulphur content on the diesel fuel is directly linked to the production of pollution. Therefore, the standard regulation has been enforced to control the sulphur content of diesel.

Starting from 1993, the Europe Union has reduced the allowable sulphur content of the diesel fuel from 5000 ppm to 2000 ppm; meanwhile, the United States has reduced it from 5000 ppm to 500 ppm (European Union, 1993). This level is set according to the capability of fuel refiner and current vehicle. Thus, the regulation took a long period for full implementation with some amendment and is continuously stringent. In 2001, the United States reported the exhaust catalytic converter damages due to the current level of sulphur content (40 CFR Parts 60 et al., 2001). Thus, the sulphur content was drastically reduced from 500 ppm to less than 15 ppm in the United States. In the European Union country, the reduction of sulphur content was made gradually, as shown in Figure 2.3. Since the regulation was implemented in 1993, the sulphur content limit was set below 2000 ppm. It was reduced gradually to 500 ppm in 1996, 350 ppm in 2000, 50 ppm in 2005 and 10 ppm in 2009 which was the Ultra-Low Sulphur Diesel (ULSD) (European Union, 1993, 1998, 2009b).

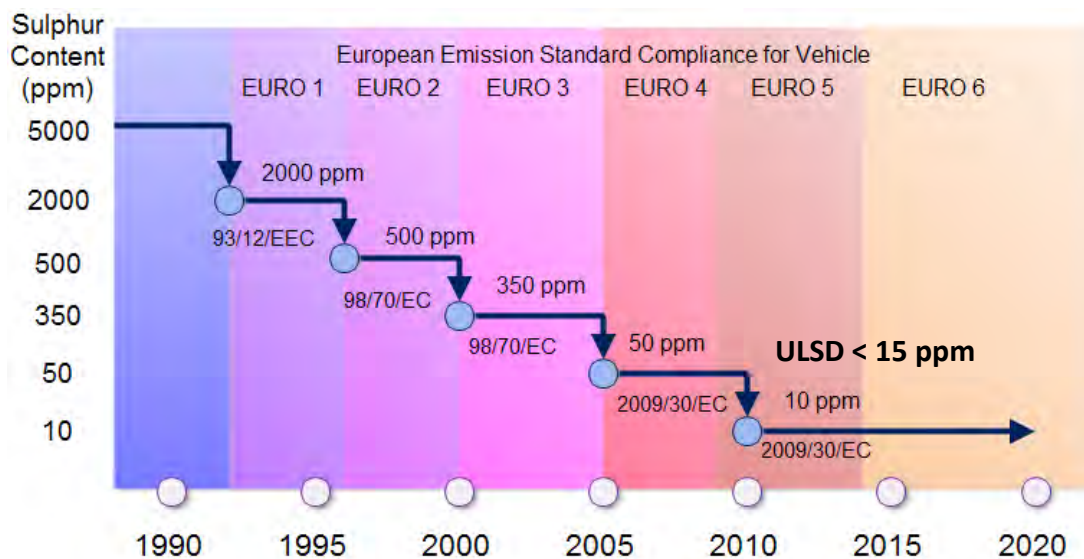


Figure 2.3: Diesel sulphur content according to the European Emission Standard

Besides lowering its sulphur content, an improvement of the diesel fuel has been made by blending it with biodiesel, which is derived from animal fat or vegetable oil. Biodiesel fuel for a vehicle was introduced in 2005 to promote renewable fuel for transportation in the United States and European Union countries (42 USC 15801, 2005; European Union, 2003). 100% biodiesel fuel for fuelling a vehicle has faced a challenge due to its limitation. Besides the climate and engine design factors, 100 % biodiesel fuel is acidic and contains particle which damages the engine component. A high cost is needed to refine this fuel for vehicle use. Some country such as the United States provides 99.99 % biodiesel fuel for the vehicle due to incentive given by the government to the refiner. However, some country blends the biodiesel with petrodiesel with a certain portion and gradually increasing it depending on the engine capability. Diesel blended with biodiesel was implemented by the European Union in 2005 by mixing 2 % biodiesel with diesel fuel and known as diesel B2. According to the plan, the implementation of diesel B5 was scheduled in 2010, but it was done earlier as it has shown positive feedback. Later in 2009, diesel B7 was introduced and immediately implemented until today (European Union, 2003, 2009b).

In Malaysia, biodiesel is derived from palm oil which is the second largest commodity after petroleum. The crude palm oil is refined to get Palm Methyl Ester (PME) which is a fuel agent. The implementation of diesel-biodiesel blend in Malaysia started with diesel B5 in 2014, diesel B7 in 2015, and diesel B10 in 2019 (The Star, 2019). As it is blended with biodiesel, this fuel is still recognized as diesel fuel and should meet the local standard regulation. In the standard, the main properties concerns are Cetane number, density, distillation point and sulphur content so that it is safe and suitable to use for the vehicle. Table 2.1 shows the properties of diesel fuel with various biodiesel blends in Malaysia.

Table 2.1: Diesel fuel properties by various blends in Malaysia (Malaysian Standard, 2014; Petron Malaysia, 2014; Petronas Dagangan Berhad, 2005)

Properties	Standards Malaysia (EURO 2M)	Petronas High-Speed Diesel	Petronas Dynamic Diesel (Euro 2M)	Petron Diesel MAX (EURO 2M)
Diesel Type	N/A	Diesel	Diesel B5	Diesel B7
Cetane Number	> 49	55	49	54
Ash, Mass %	< 0.01	0.002	0.01	<0.01
Pour Point, °C	< 19	9	15	9
Flash Point, °C	> 60	91	60	63
Kinematic Viscosity at 40 °C, mm ² /s	1.5 – 5.8	4.0	1.5-5.8	2.9
Copper Corrosion (3 h at 100 °C)	< 1	1	1	1
Density at 15 °C, kg/l	0.810 – 0.870	0.8443	0.810-0.870	0.8314
Acid Number, mg KOH/g	< 0.25	0.1	0.25	-
Electrical Conductivity, pS/m	> 50	-	50	243
Distillation at 95%, °C	< 370	365.7	370	369
Total Sulphur, mg/kg	< 50	-	500	330
Lubricity, µm	< 460	-	460	240

2.3 CNG as Alternative Fuel

Natural gas is a by-product from upstream petroleum activity. It is trapped between the layer of rock and crude oil, and these layers should be penetrated to harvest the

crude oil, as shown in Figure 2.4. At the beginning of petroleum production, the trapped natural gas was released as waste or flared because it contains a harmful gas such as methane which pollutes the environment. After a few decades, the natural gas was refined as a by-product and utilized as fuel (Speight, 2007).

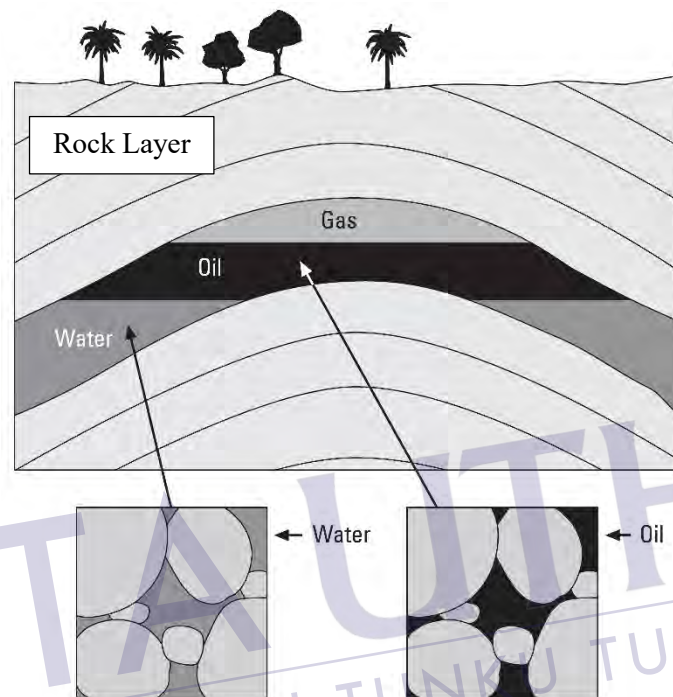


Figure 2.4: Natural gas layer in petroleum reservoir (Chandra, 2006)

The natural gas composition contains up to 80% of methane (CH_4), followed by ethane (C_2H_6), propane (C_3H_8), butane (C_4H_{10}), pentane (C_5H_{12}), and other inert gases. It has lower carbon to hydrogen ratio compared to gasoline (C_8H_{18}) and diesel ($\text{C}_{12}\text{H}_{24}$). Thus, it produces lower CO_2 emission than gasoline and diesel. It has a lower density than air and typically stored at high pressure and called as Compressed Natural Gas (CNG).

OPEC has reported that the world proven natural gas had been encouragingly increasing from 1960 to 2017. On the other hand, the world natural gas demand was also increasing but still low compared to its production. In 2017, the world proven natural gas recorded was 199.4 trillion meter cubic while the world natural gas demand was 3.7 trillion meter cubic. The significant difference between reserve and demand

was 195.7 trillion meter cubic proving that the natural gas was abundant and capable to be sustained for an extended period. Natural gas is mainly utilized for power generation, and its demand is expected to continuously increase. However, sustainable energy policy by worldwide countries may reduce the natural gas demand since it promotes the utilization of renewable energy and reduces dependency on fossil fuel, as shown in Figure 2.5 (IEA, 2018). Since the natural gas reserve is still increasing, the decrement of its demand may lead to the over-abundance crisis for the next decades. Therefore, a new policy scenario was simulated by IEA to rebalance its supply and demand. This policy enhances the natural gas utilization in power, industrial, and transportation sectors by switching coal and oil to natural gas.

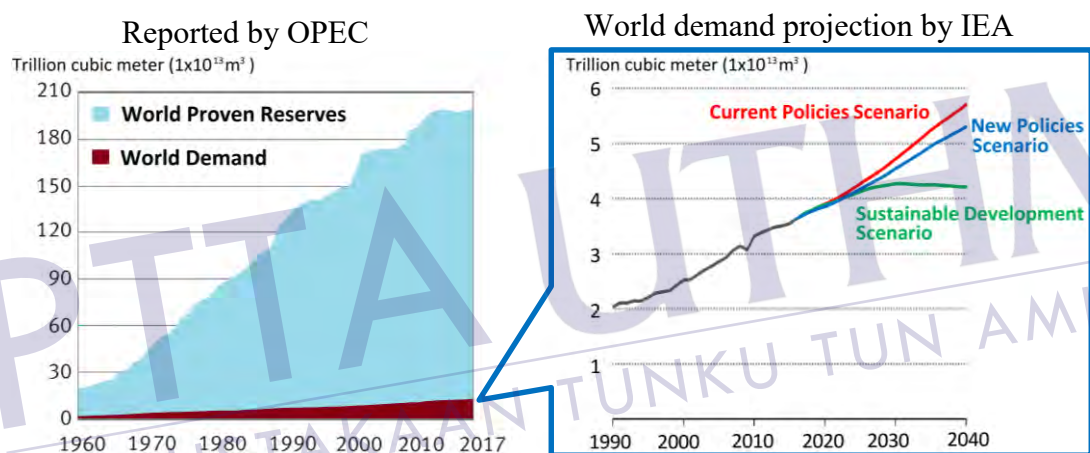


Figure 2.5: World proven natural gas reserves and demand (IEA, 2018; OPEC, 2018)

CNG fuel is widely utilized for power generation in the gas turbine engine. As it is abundant and has lower CO₂ emission, it is preferred as an alternative for fuelling an internal combustion engine. CNG has a high Rating Octane Number (RON) which is up to 120 and suitable for an SI engine. Thus, it can be applied on a dedicated gasoline engine by an additional gas fuel system and called as a bi-fuel system. This system is capable of switching either to gasoline or CNG fuel mode and suitable for vehicle purposes. A study conducted by Aslam et al. (2006) using a CNG retrofit kit on a gasoline engine shows that the CNG engine emitted less CO₂, CO and HC emissions than the gasoline engine. However, the NO_x emission for the CNG engine was higher than the gasoline engine. Another study was done by Honda Research and Development using a special ECU for a CNG fuel system. This study shows that the

CNG engine had lower performance than the gasoline engine with a 12 % power reduction and 13 % torque reduction (Yamamoto et al., 1994).

The CNG fuel application on a diesel engine is not straight forward. It is unable to self-ignite by the compression and demand a source of ignition for combustion. An existing diesel engine was converted to the CNG engine by removing an original diesel fuel system and replaced by a gas fuel system. A major modification was done by altering compression ratio (to suit with the CNG fuel for knock avoidance) and ignition system installation (Raine et al., 1988). The conversion process was irreversible and only allowed the engine to operate by a single type of fuel. Thus, the system is called a mono-fuel system. A study done by Azmir et al. (2013) shows that the CNG engine performance was lower than the diesel engine. Although the CO₂ emission was 38 % lower, the HC, CO and NO_x emission were higher than the diesel engine.

The CNG mono-fuel system shows several disadvantages as an alternative for a diesel engine. A high investment is needed for the engine conversion, and it limits the fuel type usage (Chouykerd et al., 2008). Therefore, a DDF system is preferred to be applied for fuelling the CNG fuel on the diesel engine. This system uses CNG as the main fuel and ignited by a portion of the diesel fuel. This system is more practical and economical than the mono-fuel system. It is able to perform either with the DDF system or diesel mono-fuel system, and the conversion consists of an additional gas fuel system without modifying the existing engine system or geometry.

2.4 DDF Engine

DDF engine is an alternative way for fuelling the CNG fuel on a dedicated diesel engine. Since the CNG fuel needs a source of ignition for combustion, a small amount of diesel fuel is used as the igniter. The system operates by supplying a portion of the CNG fuel into the intake manifold either by using induction or injection method. The CNG fuel is premixed with air in the intake manifold before entering the cylinder. The air-fuel mixture is compressed in the cylinder, and the diesel fuel is injected to ignite the combustion. Therefore, this engine comprises the Otto cycle and Diesel cycle (Weaver & Turner, 1994).

The DDF engine conversion on the dedicated diesel engine is straight-forward. It can be achieved by installing an additional gas fuel system without altering the original engine geometry. The CNG fuel can be supplied by induction method using a gas mixer or injection method using a gas injector at the intake manifold. The compression ratio of the engine is maintained to ensure self-ignition of the diesel fuel. This simple conversion process makes it easier and economical than a CNG mono-fuel system. Christopher S. Weaver (1994) stated that the DDF engine is highly useful because its operation is interchangeable either diesel single fuel or DDF mode. It provides a benefit when it operates at the lack of CNG supply area and makes it more convenient than the CNG mono-fuel system. Compared to a diesel engine, the DDF engine promotes lower soot emissions and becomes an alternative for ULSD (Mattson et al., 2018).

Previous studies have shown that the DDF engine performance is comparable to the diesel engine and promotes lower CO₂ and NO_x emissions at a certain condition, such as fuel ratio and engine speed (Ismail et al., 2018). It can be better or worse than the diesel engine due to several factors. According to several studies, the factors affecting the DDF engine performance and emissions are diesel to CNG fuel ratio, diesel injection timing, diesel injection quantity, intake temperature and the others.

2.4.1 DDF Engine Performance

Brake Specific Fuel Consumption (BSFC) is one of the common practice to compare the engine performance between different fuels. The BSFC is calculated by dividing fuel mass flow rate respective to the brake power to obtain fuel mass consumed to produce 1 kW.h of power. Most of the studies have shown that the fuel consumption of a DDF engine is higher than a diesel engine (Karagöz et al., 2016; Lounici et al., 2014; Papagiannakis & Hountalas, 2004). The poor utilization of the gaseous fuel is observed by a high HC and CO emissions (Lounici et al., 2014). However, an improvement of fuel utilization is observed at higher engine load where less fuel is consumed to generate the brake power.

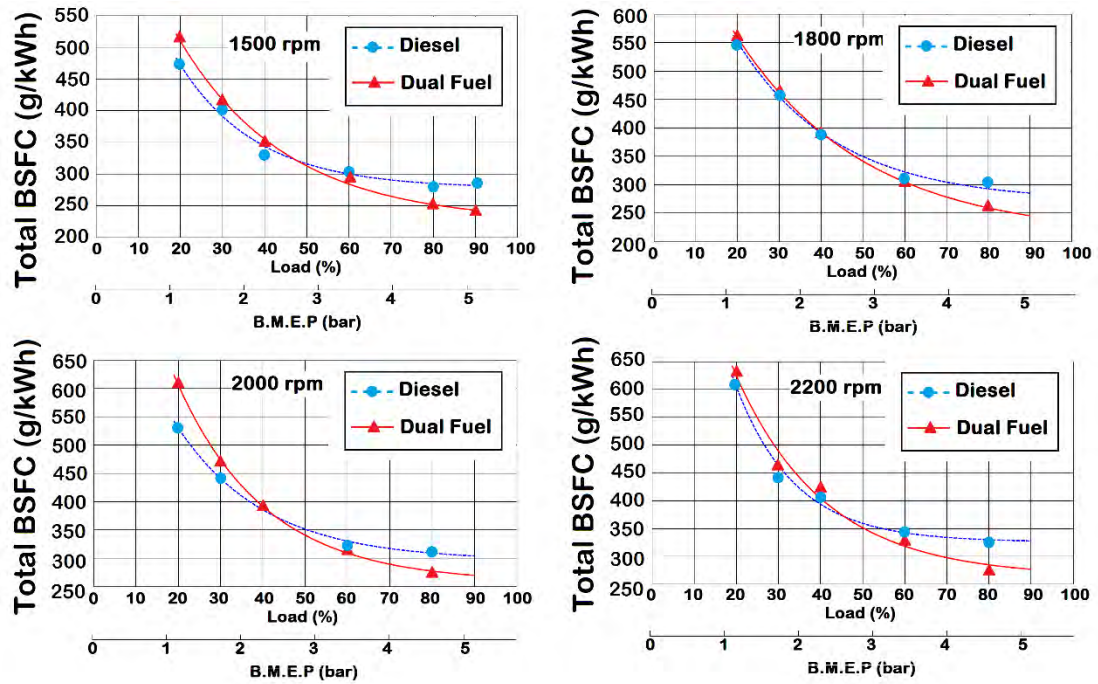


Figure 2.6: Total BSFC against engine load at various engine speeds (Lounici et al., 2014)

Since the DDF engine uses different fuels with different calorific values, Brake Specific Energy Consumption (BSEC) is preferred to be used to compare the engine performance (Misra & Murthy, 2011; Ryu, 2013a, 2013b). The BSEC is calculated using the following equation:

$$BSFC = \frac{\dot{m}}{\text{Power}} \quad (2.1)$$

$$BSEC = \frac{\dot{m} \times CV}{\text{Power}} \quad (2.2)$$

$$= \frac{\dot{m}_{\text{Diesel}} \times CV_{\text{Diesel}} + \dot{m}_{\text{CNG}} \times CV_{\text{CNG}}}{\text{Power}} \quad (2.3)$$

Where,

$$\dot{m} = \text{Mass flow rate} \quad (2.4)$$

$$CV = \text{Calorific value} \quad (2.5)$$

A study done by Ryu (2013b) showed that the BSEC for the DDF engine was higher than the diesel engine. The study was done at 1800 rpm engine speed across the engine load. The BSEC for the DDF engine was significantly higher than the diesel engine at low engine load. When the engine load was increased, the BSEC for the DDF engine was slightly higher than the diesel engine. In this study, the equivalent ratio was not kept constant across the engine load and made it incomparable.

In the author's previous study, the air-fuel ratio was kept constant across the engine speed with various diesel to CNG fuel ratio tested. As shown in Figure 2.7, the BSEC for the DDF engine is mostly higher than the diesel engine against the engine speed. However, the BSEC for the DDF engine is slightly lower than the diesel engine at 2500 rpm engine speed using 70:30 diesel to CNG fuel ratio. It shows that 30 % of CNG fuel mass fraction is able to improve the DDF engine performance at certain engine speed and the DDF engine has a potential to be an alternative for a diesel engine by controlling its fuel ratio (Ismail et al., 2018).

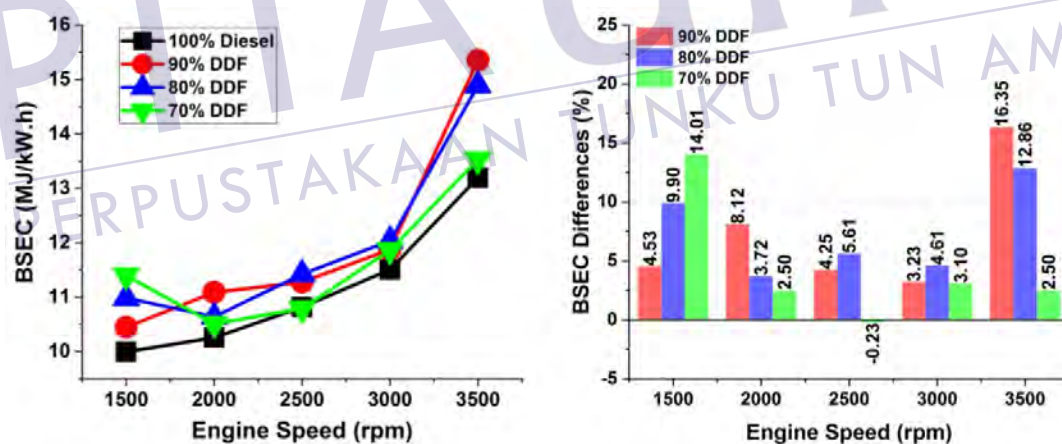


Figure 2.7: BSEC between the DDF engine and diesel engine (Ismail et al., 2018)

On the other hand, BTE is used to determine the energy balance of the engine. This parameter indicates the efficiency of fuel burned to produce a brake power. A study done by Karagöz et al. (2016) showed that the BTE of the DDF engine was lower than the diesel engine, as shown in Figure 2.8. The experiment was done at a constant 1500 rpm engine speed with the various CNG fuel fractions. It showed that 15 % of

the CNG fuel fraction leads to a significant reduction of BTE; however, it was improved with further increment of the CNG fuel fraction.

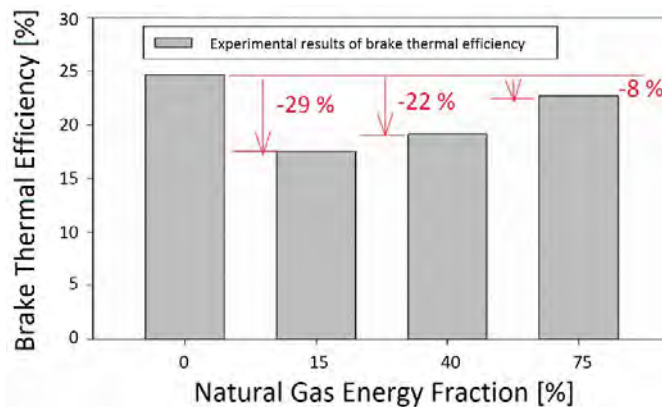


Figure 2.8: BTE at various CNG fuel fractions (Karagöz et al., 2016)

Based on the previous study, the CNG fuel fraction increment improves the DDF engine performance even lower than a diesel engine. A study of the CNG fuel fraction and equivalence ratio was done by Vávra et al. (2017) as depicted in Figure 2.9. The experiment was done at 1500 rpm engine speed with various CNG fuel fraction and equivalent ratio. At stoichiometric condition, Indicated Mean Effective Pressure (IMEP) was increased with the increment of the CNG fuel fraction. When the equivalent ratio was lean, the IMEP was retarded and slightly decreased in respect to the increment of the CNG fuel fraction. The DDF engine efficiency was lower than the diesel engine, and the increment of CNG fuel fraction led to a reduction of its efficiency. As shown in the figure, smoke emission for the DDF engine is higher than the diesel engine. The smoke emission increased when the equivalent ratio was close to stoichiometric. When the CNG fuel fraction was increased, a significant increment of smoke emission appeared to be in between 20 % and 50 % CNG fuel fraction at stoichiometric. However, the smoke emission decreased when the CNG fuel fraction exceeded 50 %.

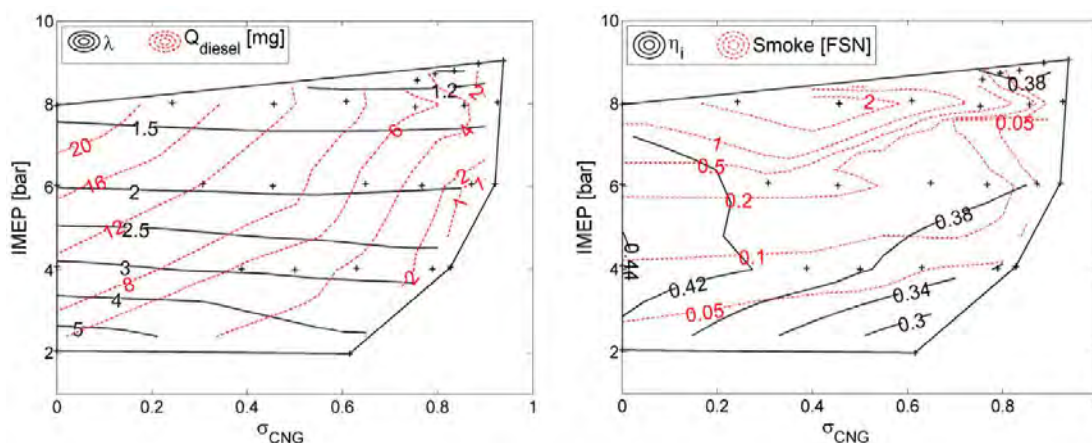


Figure 2.9: DDF engine efficiency and smoke emission across IMEP and fuel ratio (Vávra et al., 2017)

2.4.2 DDF Engine Combustion

According to Christopher S. Weaver (1994), DDF engine combustion is a combination of the Diesel cycle and Otto cycle. Several factors which influence the quality of combustion are engine load, pilot injection timing, pilot injection pressure, and fuel ratio of diesel and CNG. The combustion duration and its intensity are estimated from the heat release rate diagram, which is the most valuable information for the engine combustion (Heywood, 1988).

The study conducted by Papagiannakis & Hountalas (2004) showed that in-cylinder pressure for a DDF engine was lower than a diesel engine. However, Lounici et al., (2014) and Selim (2001) showed that the in-cylinder pressure and heat release rate for the DDF engine was lower than the diesel engine at low-load and low-speed engine operation. When the engine speed was increased, the in-cylinder pressure and heat release rate for the DDF engine was higher than the diesel engine. At high-load engine operation, in-cylinder pressure and heat release rate for DDF engine were higher than the diesel engine for both low-speed and high-speed. The comparison of the in-cylinder pressure and heat release rate between the DDF engine and diesel engine are tabulated in Table 2.2.

Table 2.2: In-cylinder pressure and heat release rate comparison of a DDF engine to diesel engine (Lounici et al., 2014; Selim, 2001)

In-Cylinder Pressure and Heat Release Rate		
Engine Operation	Low Speed	High Speed
Low Load	DDF engine was lower than the diesel engine	DDF engine was higher than the diesel engine
High Load	DDF engine was higher than the diesel engine	DDF engine was higher than the diesel engine

In-cylinder pressure and heat release rate for the DDF combustion compared to the diesel combustion are fluctuated against the combustion phases, as shown in Figure 2.10. During the compression stroke, in-cylinder pressure for the DDF engine was lower than the diesel engine. The lower in-cylinder pressure during compression stroke for the DDF engine was due to the higher specific heat capacity of CNG and air mixture. At the initial stage of the combustion stroke, the DDF engine combustion was retarded by a few degree crank angle, but it released significant higher energy than the diesel engine. However, the combustion duration for the DDF engine was shorter than the diesel engine.

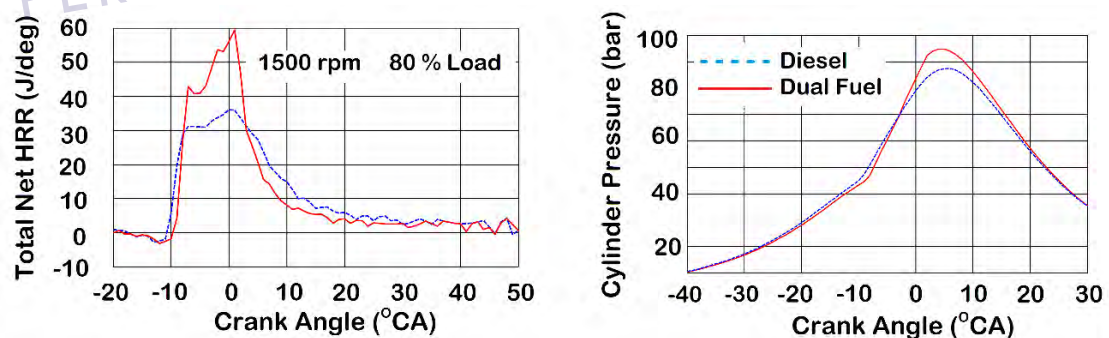


Figure 2.10: In-cylinder pressure and heat release rate for diesel engine and DDF engine (Lounici et al., 2014)

Effect of diesel injection timing on the DDF combustion was investigated at constant engine speed, load and fuel quantity (Aroonsrisopon et al., 2009; Ryu, 2013b; Selim, 2001; Zhang et al., 2015). According to the results, pressure rise rate and heat

release rate were increased against the diesel injection timing advancement. An early diesel fuel injection at low in-cylinder pressure prolonged ignition delay resulting in increased pressure rise rate and heat release rate. As shown in Figure 2.11, pressure rise rate for the DDF and diesel engine are almost similar between -20 °CA and -28 °CA; however, pressure rise rate for the DDF engine is significantly higher than the diesel engine when the diesel injection timing exceeds -30 °CA. It is because of the presence of methane in fuel mixture that prolongs ignition delay and increases the pressure rise rate (Selim, 2001).

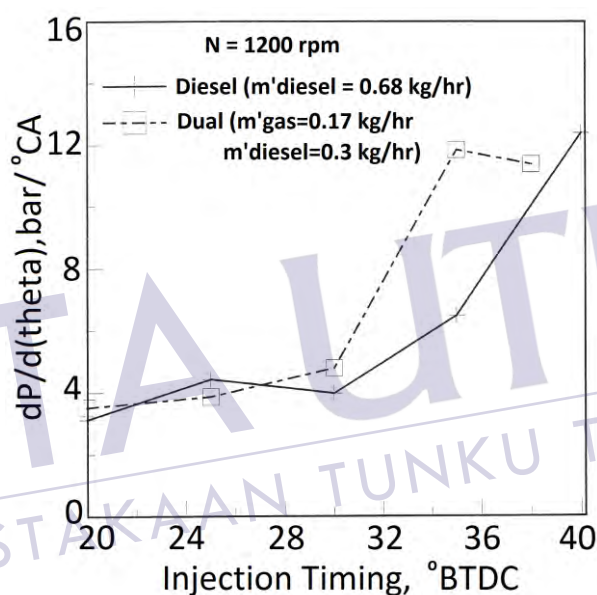


Figure 2.11: Pressure rise rate against pilot injection timing for diesel and DDF engine (Selim, 2001)

Over-advancement of diesel injection timing has led to misfire combustion. A study conducted by Aroonsrisopon et al. (2009) stated that the misfired combustion occurred in several engine cycles when the diesel fuel injection timing was at -45 °CA. When it was retarded to -30 °CA, an early start of combustion was observed by maximum in-cylinder pressure. Ryu (2013b) suggested that the IMEP should be increased against the diesel injection timing advancement. The highest IMEP was found when the diesel injection timing was at -23 °CA and this is almost similar to the study by Aroonsrisopon et al. (2009).

In another case, double-pulse diesel injection timing was introduced using first diesel injection at -45°CA with various second-pulse diesel injection timing from -38°CA to -10°CA (Aroonsrisopon et al., 2009). The stable engine operation was found when the second pulse diesel injection timing was at -30°CA ; however, it drastically increased the NO_x emission. The unstable engine operation was found when the second-pulse diesel injection timing was retarded after -20°CA . The late diesel fuel injection retards fuel vaporization and air-fuel mixture resulting in poor combustion and exhaust emissions.

Effect of diesel injection pressure on a DDF engine was studied by Ryu (2013a) and Zhang et al. (2015). It showed that the increment of diesel injection pressure improves combustion and IMEP on the DDF engine. When the diesel injection pressure was increased, better fuel atomization occurred and improved the ignition process. It fastens the combustion and increases the heat release rate.

Fuel ratio of diesel fuel to CNG fuel is the main factor that affects combustion. In actual practice, the fuel ratio for the DDF engine does not necessarily need to be constant but is specified to the engine speed and load. In term of its ignitability on a stock diesel engine, 30:70 of diesel fuel to CNG fuel ratio is easy to be combusted (Zulkifli et al., 2015). Another study shows that it is possible to obtain up to 90 % of CNG fuel fraction with higher power output than the diesel engine (Dahodwala et al., 2014; Lim et al., 2012).

Wannatong et al. (2007), Zhang et al., (2015) and Karagöz et al. (2016) demonstrated that in-cylinder pressure increased respectively with the CNG fuel fraction increment. However, the in-cylinder pressure dropped when the CNG fuel fraction reached 86 %, as shown in Figure 2.12. When the CNG fuel fraction reached the limit, the combustion characteristic changed. Besides retarded ignition delay, the premixed and mixing-controlled combustion phases were unrecognizable. When the CNG fuel fraction was below the limit, the ignition delay was shortened against the CNG fuel increment, but an excessive CNG fuel fraction led to the knock phenomenon occurrence.

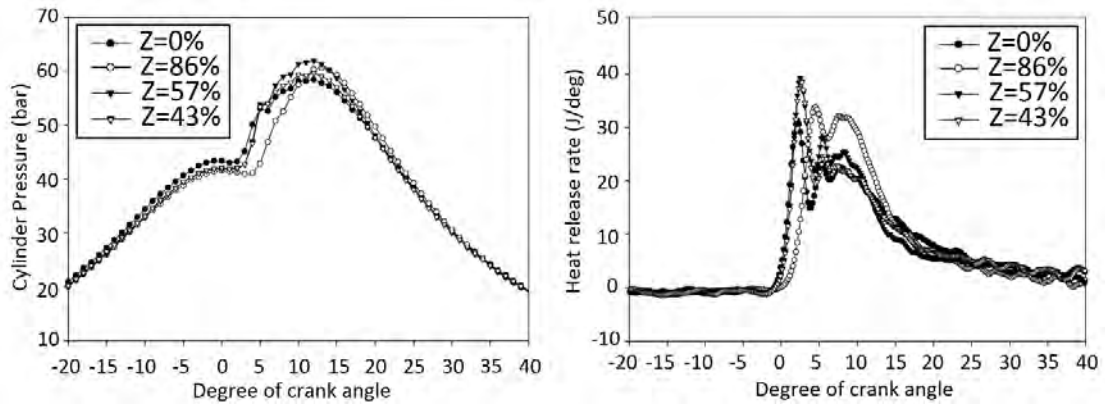


Figure 2.12: DDF combustion against CNG fuel fraction (Wannatong et al., 2007)

An experiment conducted in a constant volume chamber showed that the increment of CNG fuel fraction increases in-cylinder peak pressure, speed heat release rate and shortens combustion duration. However, it drops when the CNG fuel fraction is over than 40 % (Firmansyah et al., 2017, 2015). As shown in Figure 2.13, in-cylinder pressure was increased against the CNG fuel fraction increment from 0 % to 40 %. However, ignition delay started to prolong at the 40 % CNG fuel fraction. In-cylinder pressure was slightly decreased at the 50 % CNG fuel fraction, but ignition delay was significantly high.

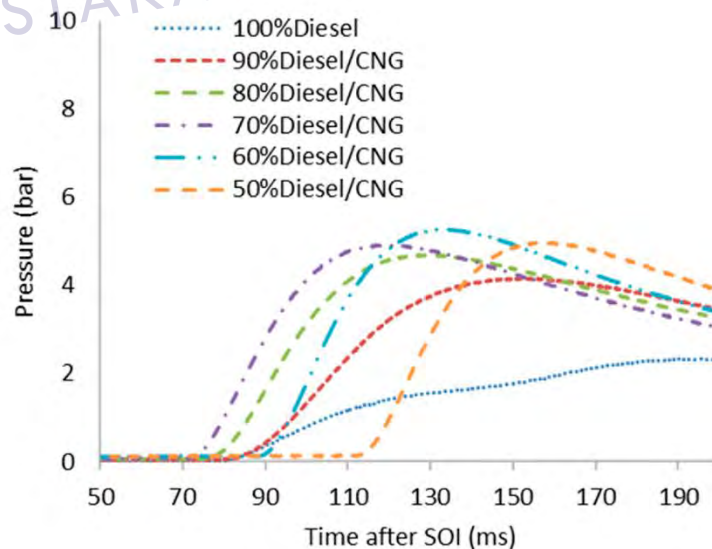


Figure 2.13: In-cylinder pressure at various fuel ratios in a constant volume chamber (Firmansyah et al., 2017)

In the same study, high-speed combustion images were photographed to investigate the combustion phase for the DDF combustion, as shown in Figure 2.14 (Firmansyah et al., 2015, 2017). According to the figure, the diesel fuel combustion shows diffusion flame and occurs in a long duration; meanwhile, the DDF combustion shows a bright spot flame with a short duration. It yields a scattered hotspot and could increase heat release rate four times faster than the diesel combustion. The scattered hotspot is formed by the diesel fuel which is distributed due to the CNG fuel combustion. The CNG fuel combustion suppresses and delays the diesel fuel combustion until it is scattered inside the chamber. This scattered fuel yields a multi-ignition point inside the cylinder.

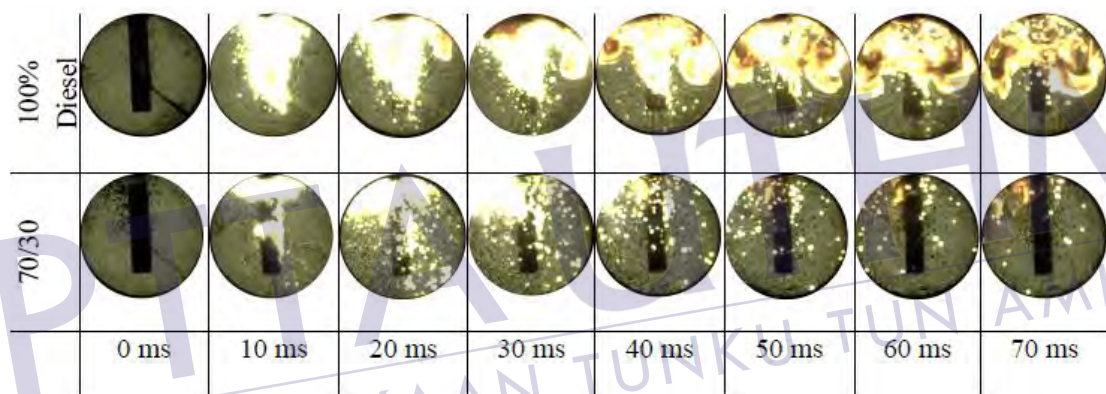


Figure 2.14: Photography image of the DDF and diesel fuel combustion (Firmansyah et al., 2015, 2017)

On the other hand, the DDF engine combustion with constant diesel fuel was experimented by Shioji et al. (2001), as shown in Figure 2.15. The experiment was conducted using a fixed diesel fuel quantity, and the CNG fuel quantity was regulated to reach the desired equivalence ratio. This study showed that the heat release rate increased against the equivalence ratio increment. The shape of the heat release rate graph for the DDF combustion and diesel combustion was quite identical when the equivalence ratio was at 0.5 and below. At equivalence ratio above 0.5, the heat release rate graph showed a significant increment of heat release rate during the mixing-controlled combustion phase. A sharp spike of heat release rate at equivalence ratio of 0.90 indicated that rapid combustion occurred at the mixing-controlled combustion

phase. According to this study, Shioji et al. (2001) stated that a high-frequency vibration was detected during the experiment and due to the knock phenomenon occurrence. It was unable to be seen in the plotted graph due the sample was averaged from 25 combustion cycles.

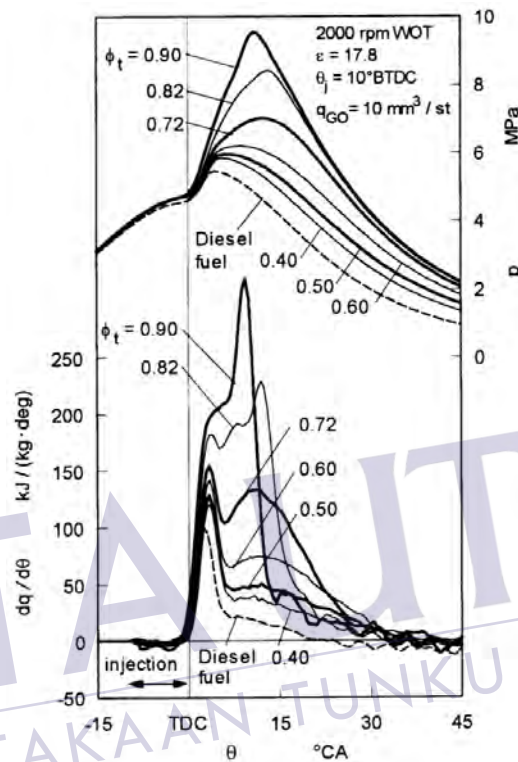


Figure 2.15: DDF engine combustion at various equivalence ratios (Shioji et al., 2001)

The previous study reported that stoichiometric combustion of the DDF engine was less efficient than the diesel engine due to deterioration of chemical efficiency and higher heat losses to the cylinder wall (Vávra et al., 2017). During the stoichiometric condition, maximizing CNG fuel fraction led to the temperature increase and exceeded the reliable limit of the diesel injector operation. The diesel injector tip was overheated and led to coking and fouling. The wear assessment study on the diesel injector tips was done at the stoichiometric condition and showed the increment of CNG fuel fraction increased the diesel injector tip temperature, as shown in Figure 2.16. When the CNG fuel fraction decreased, the diesel injector tip temperature was also decreased. The diesel injector tip temperature after 2925 second was not measured because the

REFERENCES

- 40 CFR Part 80. (2010). Regulation of Fuels and Fuel Additives: Changes to Renewable Fuel Standard Program; Final Rule. In *Federal Register* (Vol. 75, Issue 58, pp. 14669–15320). Environmental Protection Agency (EPA). <http://www.regulations.gov>
- 40 CFR Part 80. (2012a). Regulation of Fuels and Fuel Additives: 2012 Renewable Fuel Standards; Final Rule. In *Federal Register* (Vol. 77, Issue 5, pp. 1320–1358). Environmental Protection Agency (EPA). <https://doi.org/10.1111/j.1365-2753.2009.01147.x>
- 40 CFR Part 80. (2012b). Regulation of Fuels and Fuel Additives: 2013 Biomass-Based Diesel Renewable Fuel Volume. In *Federal Register* (Vol. 77, Issue 188, pp. 59458–59485). Environmental Protection Agency (EPA). <https://doi.org/10.1111/j.1365-2753.2009.01147.x>
- 40 CFR Part 80. (2013). Regulation of Fuels and Fuel Additives: Changes to Renewable Fuel Standard Program; Final Rule. In *Federal Register* (Vol. 78, Issue 158, pp. 49794–49830). Environmental Protection Agency (EPA). <https://doi.org/10.1111/j.1365-2753.2009.01147.x>
- 40 CFR Part 80. (2016). Renewable Fuel Standard Program: Standards for 2017 and Biomass-Based Diesel Volume for 2018. In *Federal Register* (Vol. 81, Issue 238, pp. 89746–89804). Environmental Protection Agency (EPA). <https://doi.org/10.1021/ac202903d>
- 40 CFR Part 80. (2017). Renewable Fuel Standard Program: Standards for 2018 and Biomass-Based Diesel Volume for 2019. In *Federal Register* (Vol. 82, Issue 237, pp. 58486–58527). Environmental Protection Agency (EPA). <http://www.regulations.gov>
- 40 CFR Parts 60, 80, & 86. (2001). Control of Air Pollution From New Motor Vehicles: Heavy-Duty Engine and Vehicle Standards and Highway Diesel Fuel



PTTA UTM
PERPUSTAKAAN TUNJUNGU TUN AMINAH

Sulfur Control Requirements; Final Rule. In *Federal Register* (Vol. 66, Issue 12 II, pp. 5002–5193). Environmental Protection Agency (EPA). <http://www.epa.gov/fedrgstr/>

42 USC 15801. (2005). Energy Policy Act of 2005. In *Public Law 109-58-Aug. 8: Vol. 119 Stat.* (Issue 594). Authenticated U.S. Government Information.

Abhijit, & Naber, J. (2008). Ionization signal response during combustion knock and comparison to cylinder pressure for SI engines. *SAE International Journal of Passenger Cars - Electronic and Electrical Systems*, 1(1), 2008-01–0981. <https://doi.org/10.4271/2008-01-0981>

Akimoto, K., Komatsu, H., & Kurauchi, A. (2013). Development of Pattern Recognition Knock Detection System using Short-time Fourier Transform. *IFAC Proceedings Volumes*, 46(21), 366–371. <https://doi.org/10.3182/20130904-4-JP-2042.00031>

Alicat Scientific. (2016). *Technical Data for Alicat M-Series Mass Flow Meters*. Alicat Scientific. www.alicat.com/m

Amann, M., Alger, T., & Mehta, D. (2011a). Engine Operating Condition and Gasoline Fuel Composition Effects on Low-Speed Pre-Ignition in High-Performance Spark Ignited Gasoline Engines. *SAE International Journal of Engines*, 4(1), 2011-01–0342. <https://doi.org/10.4271/2011-01-0342>

Amann, M., Alger, T., & Mehta, D. (2011b). The Effect of EGR on Low-Speed Pre-Ignition in Boosted SI Engines. *SAE International Journal of Engines*, 4(1), 2011-01–0339. <https://doi.org/10.4271/2011-01-0339>

Ando, H., Takemura, J., & Koujina, E. (1989). A knock anticipating strategy basing on the real-time combustion mode analysis. *SAE Technical Paper Series*, 1. <https://doi.org/10.4271/890882>

Ängeby, J., Johnsson, A., & Hellström, K. (2018). Knock detection using multiple indicators and a classification approach. *IFAC-PapersOnLine*, 51(31), 297–302. <https://doi.org/10.1016/j.ifacol.2018.10.063>

Aroonsrisopon, T., Salad, M., Wirojsakunchai, E., Wannatong, K., Siangsantorh, S., & Akarapanjavit, N. (2009, June 15). Injection Strategies for Operational Improvement of Diesel Dual Fuel Engines under Low Load Conditions. *SAE*



International. <https://doi.org/10.4271/2009-01-1855>

- Arrigoni, V., Calvi, G. F., Gaetani, B., Giavazzi, F., & Zanoni, G. F. (1978). Recent advances in the detection of knock in S.I. engines. *SAE Technical Paper Series, 1*. <https://doi.org/10.4271/780153>
- Aslam, M., Masjuki, H., Kalam, M., Abdessalam, H., Mahlia, T., & Amalina, M. (2006). An experimental investigation of CNG as an alternative fuel for a retrofitted gasoline vehicle. *Fuel, 85*(5–6), 717–724. <https://doi.org/10.1016/j.fuel.2005.09.004>
- Azimov, U., Tomita, E., & Kawahar, N. (2013). Combustion and Exhaust Emission Characteristics of Diesel Micro-Pilot Ignited Dual-Fuel Engine. In *Diesel Engine - Combustion, Emissions and Condition Monitoring*. InTech. <https://doi.org/10.5772/54613>
- Azmir, O. S., Alimin, A. J., Ismail, M. Y., & Hui, K. W. (2013). Performance and Emission Characteristics of Direct Injection C.I Engine Retrofitted with Mono-CNG System. *Applied Mechanics and Materials, 446–447*, 443–447. <https://doi.org/10.4028/www.scientific.net/AMM.446-447.443>
- Bares, P., Selmanaj, D., Guardiola, C., & Onder, C. (2018). A new knock event definition for knock detection and control optimization. *Applied Thermal Engineering, 131*, 80–88. <https://doi.org/10.1016/j.applthermaleng.2017.11.138>
- Bari, S., & Hossain, S. N. (2019). Performance of a diesel engine run on diesel and natural gas in dual-fuel mode of operation. *Energy Procedia, 160*, 215–222. <https://doi.org/10.1016/j.egypro.2019.02.139>
- Barton, R. K., Kenemuth, D. K., Lestz, S. S., & Meyer, W. E. (1970). Cycle-by-Cycle Variations of a Spark Ignition Engine - A Statistical Analysis. *SAE Technical Paper 700488*. <https://doi.org/10.4271/700488>
- Bi, F., Ma, T., Zhang, J., Li, L., & Shi, C. (2016). Knock detection in spark ignition engines base on complementary ensemble empirical mode decomposition-Hilbert transform. *Shock and Vibration, 2016*, 1–17. <https://doi.org/10.1155/2016/9507540>
- Bunes, O., & Einang, P. M. (2000). Comparing the Performance of the Common rail Fuel Injection System with the Traditional Injection System Using Computer



PT TAA UTM
PERPUSTAKAAN TUNGU TUNJUNG AMINAH

Aided Modelling and Simulation. *International Conference on Marine Science and Technology for Environmental Sustainability*, September. http://www.sintef.com/globalassets/upload/marintek/pdf-filer/publications/comparing-the-performance_pme.pdf

Burt, R., & Troth, K. A. (1970). Combustion knock in pre-chamber diesels. *SAE Technical Paper Series, 1*. <https://doi.org/10.4271/700490>

Chandra, V. (2006). *Fundamentals of Natural Gas: An International Perspective*. www.pennwellbooks.com

Channappagoudra, M., Ramesh, K., & G, M. (2018). Effect of Bio-CNG Flow Rate on Modified Diesel Engine Run with Dual Fuel. *International Journal of Engineering & Technology*, 7(3.34), 644. <https://doi.org/10.14419/ijet.v7i3.34.19406>

Chatlatanagulchai, W., Yaovaja, K., Rhienprayoon, S., & Wannatong, K. (2011). Fuzzy Knock Control of Diesel-Dual-Fuel Engine. *SAE Technical Paper 2011-01-0690*. <https://doi.org/10.4271/2011-01-0690>

Chen, L., Li, T., Yin, T., & Zheng, B. (2014). A predictive model for knock onset in spark-ignition engines with cooled EGR. *Energy Conversion and Management*, 87, 946–955. <https://doi.org/10.1016/j.enconman.2014.08.002>

Chouykerd, P., Laosiripojana, N., Chanchaona, S., Sorapipatana, C., & Yongchareon, W. (2008). Economical and environmental assessments of compressed natural gas for diesel vehicle in Thailand. *Songklanakarin Journal of Science and Technology*.

Chun, K. M., & Heywood, J. B. (1989). Characterization of knock in a spark-ignition engine. *SAE Technical Paper Series, 1*. <https://doi.org/10.4271/890156>

Cornetti, G. M., De Cristofaro, F., & Gozzelino, R. (1977). Engine failure and high speed knock. *SAE Technical Paper Series, 1*. <https://doi.org/10.4271/770147>

Curry, S. (1963a). A Three-Dimensional Study of Flame Propagation in a Spark Ignition Engine. *SAE Technical Paper Series 630487*. <https://doi.org/10.4271/630487>

Curry, S. (1963b). The Relationship Between Flame Propagation and Pressure Development During Knocking Combustion. *SAE Technical Paper 630095*.



PT TAAUTHM
PERPUSTAKAAN FUNKSI TAAUTHM

<https://doi.org/10.4271/630095>

Dahnz, C., Han, K.-M., Spicher, U., Magar, M., Schiessl, R., & Maas, U. (2010). Investigations on Pre-Ignition in Highly Supercharged SI Engines. *SAE International Journal of Engines*, 3(1), 2010-01-0355. <https://doi.org/10.4271/2010-01-0355>

Dahodwala, M., Joshi, S., Koehler, E. W., & Franke, M. (2014, April 1). Investigation of Diesel and CNG Combustion in a Dual Fuel Regime and as an Enabler to Achieve RCCI Combustion. *SAE International*. <https://doi.org/10.4271/2014-01-1308>

Dohle, U., Kampmann, S., Hammer, J., Wintrich, T., & Hinrichsen, C. (2004). Advanced Diesel Common Rail Systems for Future Emission Legislation. *International Conference on Automotive Technologies-ICAT*, 109–113. [http://www.icatconf.com/icat2000-2006/tr/2004/matbaa/papers/5.Claus Hinrichsen - ICAT-2004-11-26-Master.pdf](http://www.icatconf.com/icat2000-2006/tr/2004/matbaa/papers/5.Claus%20Hinrichsen%20-%20ICAT-2004-11-26-Master.pdf)

Douaud, A., & Eyzat, P. (1977). DIGITAP-An On-Line Acquisition and Processing System for Instantaneous Engine Data-Applications. *SAE Technical Paper Series*. <https://doi.org/10.4271/770218>

Dues, S. M., Adams, J. M., & Shinkle, G. A. (1990). Combustion Knock Sensing: Sensor Selection and Application Issues. *SAE Technical Paper Series*. <https://doi.org/10.4271/900488>

European Union. (1993). COUNCIL DIRECTIVE 93/12/EEC of 23 March 1993 relating to the sulphur content of certain liquid fuels. *Official Journal of the European Communities*.

European Union. (1998). DIRECTIVE 98/70/EC OF THE EUROPEAN PARLIAMENT AND OF THE COUNCIL of 13 October 1998 relating to the quality of petrol and diesel fuels and amending Council Directive 93/12/EEC. *Official Journal of the European Communities*, 58–68.

European Union. (2001). DIRECTIVE 2001/77/EC OF THE EUROPEAN PARLIAMENT AND OF THE COUNCIL of 27 September 2001 on the promotion of electricity produced from renewable energy sources in the internal electricity market. *Official Journal of the European Communities*, 33–40. <http://eur-lex.europa.eu/legal->



content/EN/ALL/;jsessionid=TQtJTDNGgM29cLQZnSp74LdRQmlMK66R3Kt16LsM7MvJwlpbXGFS!1258631382?uri=CELEX:32001L0077

- European Union. (2003). Directive 2003/30/EC of the European Parliament and of the Council of 8 May 2003 on the promotion of the use of biofuels or other renewable fuels for transport. In *Official Journal of the European Union* (pp. 42–46). <https://doi.org/10.1016/j.jclepro.2010.02.014>
- European Union. (2009a). DIRECTIVE 2009/28/EC OF THE EUROPEAN PARLIAMENT AND OF THE COUNCIL of 23 April 2009 on the promotion of the use of energy from renewable sources and amending and subsequently repealing Directives 2001/77/EC and 2003/30/EC. *Official Journal of the European Union*, 16–62.
- European Union. (2009b). Directive 2009/30/EC of the European Parliament and of the Council of 23 April 2009 amending Directive 98/70/EC as regards the specification of petrol, diesel and gas-oil and introducing a mechanism to monitor and reduce greenhouse gas emissions and amend. *Official Journal of the European Union*, 88–113.
- Felt, A. E., & Steele, W. A. (1962). Combustion Control in Dual-Fuel Engines. In *SAE Technical Papers*. <https://doi.org/10.4271/620555>
- Ferraro, C. V. (1978). A Knock Intensity Meter Based on Kinetic Criterion. *SAE Technical Paper Series, 1*. <https://doi.org/10.4271/780154>
- Firmansyah, A. Aziz, A., Heikal, M., & Zainal A., E. (2017). Diesel/CNG Mixture Autoignition Control Using Fuel Composition and Injection Gap. *Energies*, 10(10), 1639. <https://doi.org/10.3390/en10101639>
- Firmansyah, Aziz, A. R. A., & Heikal, M. R. (2015). The combustion behavior of diesel/CNG mixtures in a constant volume combustion chamber. *IOP Conference Series: Materials Science and Engineering*, 100(1), 012032. <https://doi.org/10.1088/1757-899X/100/1/012032>
- Fitton, J. C., & Nates, R. J. (1992). Investigation into the relationship between knock intensity and piston Seizure. *N&O Joernaal*.
- Flaig, U., Polach, W., & Ziegler, G. (1999). Common Rail System (CR-System) for Passenger Car DI Diesel Engines; Experiences with Applications for Series



PT TAAU THM
PERPUSTAKAAN TUNGU AMINAH

Production Projects. *International Congress and Exposition*, 724.
<https://doi.org/10.4271/1999-01-0191>

Ganesan, V. (2003). *Internal Combustion Engines* (Second Edi). Tata McGraw Hill.

Gas Malaysia. (2015). *SAFETY DATA SHEET Natural Gas*.

Gómez Montoya, J. P., Olsen, D. B., & Amell, A. A. (2018). Engine operation just above and below the knocking threshold, using a blend of biogas and natural gas. *Energy*. <https://doi.org/10.1016/j.energy.2018.04.079>

Guess, J. F. (1983). Analysis of Piezoelectric Benders Used As Knock Sensors. *SAE Technical Paper Series, 1*. <https://doi.org/10.4271/830170>

Harris, C. M., & Piersol, A. G. (2002). Harris' Shock and Vibration Handbook. In *McGraw-Hill* (5th ed.). McGraw-Hill.

Haskell, W. W., & Bame, J. L. (1965). Engine knock - an end-gas explosion. *SAE Technical Paper Series*. <https://doi.org/10.4271/650506>

Head, H. E., & Wake, J. D. (1980). Noise of Diesel Engines Under Transient Conditions. *SAE Technical Paper Series, 1*. <https://doi.org/10.4271/800404>

Heywood, J. B. (1988). *Internal Combustion Engine Fundamentals*. Mc Graw-Hill, Inc.

Huang, B., Hu, E., Huang, Z., Zheng, J., Liu, B., & Jiang, D. (2009). Cycle-by-cycle variations in a spark ignition engine fueled with natural gas-hydrogen blends combined with EGR. *International Journal of Hydrogen Energy*. <https://doi.org/10.1016/j.ijhydene.2009.08.002>

IEA. (2017). *Market Report Series: Oil 2017*. International Energy Agency (IEA). <https://www.iea.org/oilmarketreport/>

IEA. (2018). Outlook for natural gas: Excerpt from world energy outlook 2017. In *World Energy Outlook*. International Energy Agency (IEA).

Ismail, M. M., Fawzi, M., Ali, M., Fathul, A., Zulkifli, H., & Osman, S. A. (2018). Effects of fuel ratio on performance and emission of diesel-compressed natural gas (CNG) dual fuel engine. *Journal of the Society of Automotive Engineers Malaysia*, 2(2), 157–165.
<http://jsaem.saemalaysia.org.my/index.php/jsaem/article/view/21/17>

Ismail, M. M., Zulkifli, H., Fawzi, M., & Osman, S. A. (2016). Conversion Method of



a Diesel Engine to a CNG-Diesel Dual Fuel Engine and its Financial Savings. *ARPJ Journal of Engineering and Applied Sciences*, 11(8).
www.arpnjournals.com

Jamsran, N., Putrasari, Y., & Lim, O. (2016). A computational study on the autoignition characteristics of an HCCI engine fueled with natural gas. *Journal of Natural Gas Science and Engineering*.
<https://doi.org/10.1016/j.jngse.2016.01.008>

Jun, D., Ishii, K., & Iida, N. (2003). Autoignition and Combustion of Natural Gas in a 4 Stroke HCCI Engine. *JSME International Journal Series B*, 46(1), 60–67.
<https://doi.org/10.1299/jsmeb.46.60>

Kaji, K., Matsushige, S., Kanamaru, M., Takahashi, J., & Asano, S. (1986). Development of Knock Sensor. *SAE Technical Paper Series*, 1.
<https://doi.org/10.4271/861375>

Kalghatgi, G. T., & Bradley, D. (2012). Pre-ignition and ‘super-knock’ in turbo-charged spark-ignition engines. *International Journal of Engine Research*, 13(4), 399–414. <https://doi.org/10.1177/1468087411431890>

Karagöz, Y., Sandalçı, T., Koylu, U. O., Dalkılıç, A. S., & Wongwises, S. (2016). Effect of the use of natural gas–diesel fuel mixture on performance, emissions, and combustion characteristics of a compression ignition engine. *Advances in Mechanical Engineering*, 8(4), 168781401664322.
<https://doi.org/10.1177/1687814016643228>

Kubesh, J., & Brehob, D. D. (1992, October 1). Analysis of knock in a dual-fuel engine. *SAE Technical Paper 922367*. <https://doi.org/10.4271/922367>

Kumano, M., Yano, K., Nakamura, K., & Uono, H. (2006). Advanced Electronics for a Clean Diesel Engine Management System. *SAE Technical Paper 2006-21-0059*, 724.

Lee, W., & Schaefer, H. J. (1983). Analysis of local pressures, surface temperatures and engine damages under knock conditions. *SAE Technical Paper Series*, 1.
<https://doi.org/10.4271/830508>

Leppard, W. R. (1982). Individual-cylinder knock occurrence and intensity in multicylinder engines. *SAE Technical Paper Series*, 1.



<https://doi.org/10.4271/820074>

- Lim, O., Iida, N., Cho, G., & Narankhuu, J. (2012, October 23). The Research about Engine Optimization and Emission Characteristic of Dual Fuel Engine Fueled with Natural Gas and Diesel. *SAE International*. <https://doi.org/10.4271/2012-32-0008>
- Lounici, M. S., Benbellil, M. A., Loubar, K., Niculescu, D. C., & Tazerout, M. (2017). Knock characterization and development of a new knock indicator for dual-fuel engines. *Energy*, *141*, 2351–2361. <https://doi.org/10.1016/j.energy.2017.11.138>
- Lounici, M. S., Loubar, K., Tarabet, L., Balistrrou, M., Niculescu, D.-C., & Tazerout, M. (2014). Towards improvement of natural gas-diesel dual fuel mode: An experimental investigation on performance and exhaust emissions. *Energy*, *64*, 200–211. <https://doi.org/10.1016/j.energy.2013.10.091>
- Malaghan, S., Ellur, R., Alur, S. A., & Banapurmath, N. R. (2018). Effect of CNG Flow Rate and Combustion Chamber Shapes on the Performance of Dual Fuel Engine Operated with HnOME and CNG. *International Journal of Pure and Applied Mathematics*, *120*(6), 907–923.
- Malaysian Standard. (2014). MS123-1:2014. In *Malaysian Standard*. Department of Standards Malaysia. <http://www.sirim.my/srhc/documents/July-Aug-2014/14H002R1-PC.pdf>
- Male, T. (1948). Photographs at 500,000 frames per second of combustion and detonation in a reciprocating engine. *Symposium on Combustion and Flame, and Explosion Phenomena*, *3*(1), 721–726. [https://doi.org/10.1016/S1062-2896\(49\)80100-0](https://doi.org/10.1016/S1062-2896(49)80100-0)
- Mansor, W. N. W., Abdullah, S., Olsen, D. B., & Vaughn, J. S. (2018). Diesel-natural gas engine emissions and performance. *AIP Conference Proceedings*, *2035*, 060010. <https://doi.org/10.1063/1.5075590>
- Matekunas, F. A. (1983). Modes and Measures of Cyclic Combustion Variability. *SAE Technical Paper Series*, *1*. <https://doi.org/10.4271/830337>
- Matsumoto, S., Klose, C., & Schneider, J. (2013). 4 th Generation Diesel Common Rail System: Realizing Ideal Structure Function for Diesel Engine. *SAE Technical Paper 2013-01-1590 2012-01-1753*. <https://doi.org/10.4271/2013-01-1590>



PT TAAUTHM
PERPUSTAKAAN TUNJUKU AMINAH

1590

- Mattson, J. M. S., Langness, C., & Depcik, C. (2018). An Analysis of Dual-Fuel Combustion of Diesel with Compressed Natural Gas in a Single-Cylinder Engine. *SAE Technical Paper Series 2018-01-0248, 1*. <https://doi.org/10.4271/2018-01-0248>
- Miller, C. D. (1942). *A Study by High Speed Photography of Combustion and Knock in a Spark Ignition Engine*. National Advisory Committee for Aeronautics (NACA). <https://ntrs.nasa.gov/search.jsp?R=19930091806>
- Miller, C. D. (1947). Roles of Detonation Waves and Autoignition in Spark - Ignition Engine Knock as Shown by Photographs Taken at 40,000 and 200,000 Frames Per Sec. *SAE Technical Paper 470207*. <https://doi.org/10.4271/470207>
- Millo, F., & Ferraro, C. V. (1998). Knock in S.I. engines: A comparison between different techniques for detection and control. *SAE Technical Papers*. <https://doi.org/10.4271/982477>
- Misra, R. D., & Murthy, M. S. (2011). Performance, emission and combustion evaluation of soapnut oil–diesel blends in a compression ignition engine. *Fuel, 90*(7), 2514–2518. <https://doi.org/10.1016/j.fuel.2011.03.003>
- Mortara, W., & Canta, C. (1983). Engine Stability Sensor. *SAE Technical Paper Series, 1*. <https://doi.org/10.4271/830428>
- Nagata, Kohji, Tanaka, Y., & Yano, K. (2004). Technologies of DENSO Common Rail for Diesel Engine and Consumer Values. *SAE Technical Paper 2004-21-0075, 1–7*.
- Nagata, Koji. (2004). *State-Of-Art Technologies For Diesel Common Rail System*. <https://doi.org/10.4271/2004-28-0068>
- Nwafor, O. M. I. (2002a). Lean-knock limits for dual-fuel combustion of natural gas in diesel engine. *Indian Journal of Engineering & Materi & Sciences, 9*(4), 250–254.
- Nwafor, O. M. I. (2002b). Knock characteristics of dual-fuel combustion in diesel engines using natural gas as primary fuel. *Sadhana, 27*(3), 375–382. <https://doi.org/10.1007/BF02703658>
- Ono Sokki. (2010). *High-Precision Fuel Flow Meters*.



PT TAAUTHM
PERPUSTAKAAN TINKU TUN AMINAH

<http://www.onosokki.co.jp/English/english.htm>

OPEC. (2018). *OPEC Annual Statistical Bulletin 2018* (pp. 1–128). Organization of the Petroleum Exporting Countries (OPEC).

Ortmann, S., Rychetsky, M., Glesner, M., & Groppo, R. (1997). Engine knock detection using multi-feature classification by means of non-linear mapping. *Proceedings of {ISATA}*, 97, 607–613. <http://citeseerx.ist.psu.edu/>

Papagiannakis, R. ., & Hountalas, D. . (2004). Combustion and exhaust emission characteristics of a dual fuel compression ignition engine operated with pilot Diesel fuel and natural gas. *Energy Conversion and Management*, 45(18–19), 2971–2987. <https://doi.org/10.1016/j.enconman.2004.01.013>

Petron Malaysia. (2014). *Product Data Sheet: PETRON Diesel Max*. http://www.petron.com.my/web/Media/uploads/PDS_Petron_B7_Diesel_Max_-_with_additive_-_Dec_8_20141.pdf

Petronas Dagangan Berhad. (2005). *Product Data Sheet: DYNAMIC DIESEL (Euro 2M)*.

Priede, T. (1960). Relation between Form of Cylinder-Pressure Diagram and Noise in Diesel Engines. *Proceedings of the Institution of Mechanical Engineers: Automobile Division*, 14(1), 63–97. https://doi.org/10.1243/PIME_AUTO_1960_000_012_02

Priede, T. (1980). In Search of Origins of Engine Noise-an Historical Review. *SAE Technical Paper 800534*. <https://doi.org/10.4271/800534>

Pukelsheim, F. (1994). The three sigma rule. *The American Statistician*, 48(2), 88–91. <https://doi.org/10.1080/00031305.1994.10476030>

Pulkrabek, W. W. (2004). *Engineering Fundamentals of the Internal Combustion Engine* (2nd ed.). Pearson Prentice-Hall.

Raine, R. R., Stephenson, J., & Elder, S. T. (1988). Characteristics of Diesel Engines Converted to Spark Ignition Operation Fuelled with Natural Gas. *SAE Technical Paper 880149, 1*. <https://doi.org/10.4271/880149>

Rothrock, A. . M., Spencer, R. C., & Miller, C. D. (1941). *A High-Speed Motion-Picture Study of Normal Combustion, Knock and preignition in a Spark-Ignition Engines*. National Advisory Committee for Aeronautics (NACA).



PT TAAUTHIM
PERPUSTAKAAN TUNJUNING AMINAH

<https://ntrs.nasa.gov/search.jsp?R=19930091782>

Russell, M. F., & Haworth, R. (1985). Combustion Noise from High Speed Direct Injection Diesel Engines. *SAE Technical Paper Series, 1*.
<https://doi.org/10.4271/850973>

Ryu, K. (2013a). Effects of pilot injection pressure on the combustion and emissions characteristics in a diesel engine using biodiesel-CNG dual fuel. *Energy Conversion and Management, 76*, 506–516.
<https://doi.org/10.1016/j.enconman.2013.07.085>

Ryu, K. (2013b). Effects of pilot injection timing on the combustion and emissions characteristics in a diesel engine using biodiesel-CNG dual fuel. *Applied Energy, 111*, 721–730. <https://doi.org/10.1016/j.apenergy.2013.05.046>

SAE International. (2004). Engine Power Test Code - Spark Ignition and Compression Ignition - Net Power Rating. In *Surface Vehicle Standard*.
https://doi.org/10.4271/J1349_200403

Saidi, M. H., Far, K. E., & Pirouzpanah, V. (2005). Analysis of Combustion Process in Dual Fuel Diesel Engines: Knock Phenomenon Approach. *SAE Technical Paper 2005-01-1132*. <https://doi.org/10.4271/2005-01-1132>

Schmillen, K. P., & Rechs, M. (1991). Different methods of knock detection and knock control. *SAE Technical Paper Series*. <https://doi.org/10.4271/910858>

Scott, D. W. (1979). On optimal and data-based histograms. *Biometrika, 66*(3), 605–610. <https://doi.org/10.1093/biomet/66.3.605>

Sczomak, D. P., & Henein, N. A. (1979). Cycle-To-Cycle Variation with Low Ignition Quality Fuels in a CFR Diesel Engine. *SAE Technical Paper Series, 1*.
<https://doi.org/10.4271/790924>

Selim, M. Y. E. (2001). Pressure–time characteristics in diesel engine fueled with natural gas. *Renewable Energy, 22*, 473–489. www.elsevier.nl/locate/renene

Shioji, M., Ishiyama, T., Ikegami, M., Mitani, S., & Shibata, H. (2001). Performance and Exhaust Emissions in a Natural-Gas Fueled Dual-Fuel Engine. *JSME International Journal Series B, 44*(4), 641–648.
<https://doi.org/10.1299/jsmeb.44.641>

Speight, J. G. (2007). *Natural Gas* (1st Editio). Elsevier.



<https://doi.org/10.1016/C2013-0-15520-1>

Sremec, M., Taritaš, I., Sjerić, M., & Kozarac, D. (2017). Numerical Investigation of Injection Timing Influence on Fuel Slip and Influence of Compression Ratio on Knock Occurrence in Conventional Dual Fuel Engine. *Journal of Sustainable Development of Energy, Water and Environment Systems*, 5(4), 518–532. <https://doi.org/10.13044/j.sdewes.d5.0163>

Stalhammar, P., Erlandsson, L., & Willner, K. (2011). *Assessment of the dual fuel technology*.

Tagai, T., Ishida, M., Ueki, H., & Watanabe, T. (2003). Effects of Equivalence Ratio and Temperature of CNG Premixture on Knock Limit in a Dual Fueled Diesel Engine. *SAE Technical Paper 2003-01-1934*. <https://doi.org/10.4271/2003-01-1934>

The Star. (2019, January 18). B10 biodiesel switch mandatory. *The Star Online*. <https://www.thestar.com.my/business/business-news/2019/01/18/b10-biodiesel-switch-mandatory/>

Toyota Motor Corporation. (2007). *Toyota Hilux*.

Vávra, J., Bortel, I., Takáts, M., & Diviš, M. (2017). Emissions and performance of diesel–natural gas dual-fuel engine operated with stoichiometric mixture. *Fuel*, 208, 722–733. <https://doi.org/10.1016/j.fuel.2017.07.057>

Wang, Z., Liu, H., & Reitz, R. D. (2017). Knocking combustion in spark-ignition engines. *Progress in Energy and Combustion Science*, 61, 78–112. <https://doi.org/10.1016/j.pecs.2017.03.004>

Wang, Z., Liu, H., Song, T., Qi, Y., He, X., Shuai, S., & Wang, J. (2015). Relationship between super-knock and pre-ignition. *International Journal of Engine Research*, 16(2), 166–180. <https://doi.org/10.1177/1468087414530388>

Wang, Z., Liu, H., Song, T., Xu, Y., Wang, J.-X., Li, D.-S., & Chen, T. (2014). Investigation on Pre-ignition and Super-Knock in Highly Boosted Gasoline Direct Injection Engines. *SAE Technical Paper Series*, 1. <https://doi.org/10.4271/2014-01-1212>

Wang, Z., Qi, Y., He, X., Wang, J., Shuai, S., & Law, C. K. (2015). Analysis of pre-ignition to super-knock: Hotspot-induced deflagration to detonation. *Fuel*, 144,



PTT AUTHORITY
PERPUSTAKAAN TUNKU TUN AMINAH

222–227. <https://doi.org/10.1016/j.fuel.2014.12.061>

Wannatong, K., Akarapanyavit, N., Siengsanorh, S., & Chanchaona, S. (2007). Combustion and knock characteristics of natural gas diesel dual fuel engine. *SAE International*. <https://doi.org/10.4271/2007-01-2047>

Wattanapanichaporn, O., Jantaradach, W., Wannatong, K., & Aroonsrisopon, T. (2013). Cylinder-to-Cylinder Variations in Diesel Dual Fuel Combustion under Low-load Conditions. *Journal of Research and Applications in Mechanical Engineering (JRAME)*, 1(4), 1–8.

Weaver, C. S., & Turner, S. H. (1994, March 1). Dual Fuel Natural Gas/Diesel Engines: Technology, Performance, and Emissions. *Fuel*. <https://doi.org/10.4271/940548>

WHO. (2015). *Reducing global health risks through mitigation of short-lived climate pollutants. Scoping report for policy-makers*. World Health Organization Press. www.who.int/about/licensing/copyright_form/en/index.html

WHO. (2017). *Ten Years in Public Health 2007-2017*. World Health Organization (WHO).

Willand, J., Daniel, M., Montefrancesco, E., Geringer, B., Hofmann, P., & Kieberger, M. (2009). Limits on downsizing in spark ignition engines due to pre-ignition. *MTZ Worldwide*, 70(5), 56–61. <https://doi.org/10.1007/bf03226955>

Withrow, L., & Boyd, T. A. (1931). Photographic Flame Studies in the Gasoline Engine. *Industrial & Engineering Chemistry*, 23(5), 539–547. <https://doi.org/10.1021/ie50257a018>

Yamamoto, Y., Sato, K., Matsumoto, S., & Tsuzuki, S. (1994). Study of Combustion Characteristics of Compressed Natural Gas as Automotive Fuel. *SAE Technical Paper*. <https://doi.org/10.4271/940761>

Yaovaja, K., & Chatlatanagulchai, W. (2014). Knock control in a diesel-dual-fuel premixed-charge- compression-ignition (DF-PCCI) engine using a fuzzy supervisory system. *Kasetsart Journal - Natural Science*.

Yusaf, T., Baker, P., Hamawand, I., & Noor, M. M. (2013). Effect of Compressed Natural Gas Mixing on the Engine Performance and Emissions. *International Journal of Automotive and Mechanical Engineering*, 8(1), 1416–1429.



PTT AUTHM
PERPUSTAKAAN TUNJUN AMINAH

<https://doi.org/10.15282/ijame.8.2013.29.0117>

Zaccardi, J.-M., Duval, L., & Pagot, A. (2009). Development of Specific Tools for Analysis and Quantification of Pre-ignition in a Boosted SI Engine. *SAE International Journal of Engines*, 2(1), 2009-01–1795.

<https://doi.org/10.4271/2009-01-1795>

Zhang, Q., Li, N., & Li, M. (2015). Combustion and emission characteristics of an electronically- controlled common-rail dual-fuel engine. *Journal of the Energy Institute*. <https://doi.org/10.1016/j.joei.2015.03.012>

Żółtowski, A. (2014). Knock Combustion in Dual Fuel Diesel Engine. *Journal of KONES. Powertrain and Transport*, 21(4), 547–553.

<https://doi.org/10.5604/12314005.1130523>

Zulkifli, F. H., Fawzi, M., & Osman, S. A. (2015). A review on knock phenomena in CNG-diesel dual fuel system. *Applied Mechanics and Materials*, 773–774, 550–554. <https://doi.org/10.4028/www.scientific.net/AMM.773-774.550>



PTTA UTHM
PERPUSTAKAAN TUNKU TUN AMINAH